12/9/20-96 g SC (1)

PNNL-11182
UC-702

Predictive Calculations to Assess the Long-Term Effect of Cementitious Materials on the pH and Solubility of Uranium (VI) in a Shallow and Disposal Environment

L. J. Criscenti
R. J. Serne
K. M. Krupka
M. I. Wood

August 1996

Prepared for the U.S. Department of Energy
under Contract DE-AC06-76RLO 1830

Pacific Northwest National Laboratory
Operated for the U.S. Department of Energy
by Battelle

PNNL-11182

DISCLAIMER

PACIFIC NORTHWEST NATIONAL LABORATORY
operated by
BATTELLE
for the
UNITED STATES DEPARTMENT OF ENERGY
under Contract DE-AC06-76RLO 1830

Printed in the United States of America

Available to DOE and DOE contractors from the Office of Scientific and Technical Information, P.O. Box 62, Oak Ridge, TN 37831; prices available from (615) 576-8401.

Available to the public from the National Technical Information Service, U.S. Department of Commerce, 5285 Port Royal Rd., Springfield, VA 22161


The document was printed on recycled paper.

PNNL-11182
UC-702

Predictive Calculations to Assess the Long-Term Effect of Cementitious Materials on the pH and Solubility of Uranium(VI) in a Shallow Land Disposal Environment

L. J. Criscenti
R. J. Serne
K. M. Krupka
M. I. Wood [a]

September 1996

Prepared for
the U.S. Department of Energy
under Contract DE-AC06-76RLO 1830

Pacific Northwest National Laboratory
Richland, Washington 99352

(a) Westinghouse Hanford Company
Richland, Washington 99352

Executive Summary

One proposed method of low-level radioactive waste (LLW) disposal is to mix the radioactive waste streams with cement, place the mixture in steel barrels, and store the barrels in unsaturated near-surface sediments. Cement or concrete is frequently used in burial grounds because cement porewaters are buffered at high pH values, and typically lanthanides and actinides are very insoluble in highly alkaline environments. The calculations performed in this study demonstrate that the pH of cement porewaters will be maintained at values greater than 10 for 10,000 years (the period of regulatory concern) under hydrogeochemical conditions specific to the Hanford Site. The concentrations of dissolved hexavalent uranium [U(VI)] are also constrained by the high pH and predicted porewater compositions over the 10,000-year period, which is favorable from a long-term performance perspective.

To evaluate the potential for suppressing the release of U [specifically U(VI)] from low-level radioactive waste solidified in cement for 10,000 years at the Hanford Site, sixteen waste disposal scenarios were evaluated. These scenarios are described by the permutations of two choices for each of four variables: the recharge rate, the influent solution, the length (or number) of waste drums in the flow path, and the mass of cement per waste drum. Coupled reaction/transport calculations were performed for nine of the scenarios using the CTM (Contaminant Transport Model) computer code. Results for the other seven scenarios are deduced from these calculations.

These calculations demonstrate that the portlandite [$Ca(OH)_2$] component of the CSH-gel phase in cement disappears over time and the SiO_2 (am) component may be introduced depending on the influent composition. The cement degrades more quickly when it reacts with soil porewater with a composition typical of Trench 8 porewater than when it reacts with rainwater. The pH values drop below 10 when the calcium silicate (CaH_2SiO_4) component of CSH-gel completely dissolves.

The CTM calculations predict that, regardless of which recharge rate and influent solution is selected, solid CaH_2SiO_4 will not disappear within 10,000 years from steel barrels that are completely filled with Portland Type I cement. For a barrel that is only one-third filled with cement, the results predict that, given a 0.5 cm/yr recharge rate, the CSH-gel will not disappear in 10,000 years. On the other hand, at a recharge rate of 5 cm/yr, CSH-gel is predicted to completely dissolve after 4,000 to 8,000 years in the barrel that is only one-third filled with Portland Type I cement. If three drums were stacked on top of each other, the cement would not all dissolve and pH values would not drop below 10 for the entire 10,000 year period modeled. The upper two barrels would however be completely devoid of cementitious solids by the end of 10,000 years for this upper bound recharge rate of 5 cm/yr.

As long as cement hydration (weathering) products containing CSH-gel are present, the pH of the surrounding water will remain above 10. The most likely U(VI)-bearing solids that may precipitate from U released from the LLW waste are quite insoluble at pH values above 10. Based on the solubilities of these solids, the total concentrations of dissolved U could range from subparts per trillion ($< 10^{-12}$ mg/L) to at most one part per million (ppm, 10^{-6} mg/L) under these cement gel dominated conditions. After the cement solids have been exhausted through dissolution reactions, the total concentrations of dissolved U(VI) in the porewater would be controlled by the solubility of solids such as schoepite ($UO_3 \cdot 2H_2O$), uranyl silicates or perhaps alkaline-earth uranates. The silicates are

less soluble than the alkaline earth uranates and schoepite at slightly alkaline to neutral pH values expected at the Hanford area. Thus, U(VI) silicate solids would limit the dissolved U concentrations to the low ppb range. If present in the waste or formed in situ, calcium uranate would limit dissolved U concentrations within the range 100s of ppb to low ppm. Finally, if schoepite is the U-bearing solubility control, dissolved U concentrations would be in the range of several ppm to several tens of ppm.

Experimental studies where specific U(VI) solids have been used or identified in waters relevant to shallow land burial grounds or cement waste forms are quite limited. There is only empirical data available for U solution concentrations in the presence of cement leachates. In general, the U solution concentrations are found to be less than tens of ppb to less than one ppm, which is in good agreement with our predictions. Empirical solubility data for uranyl silicates and U(VI)-bearing solids containing alkaline-earth and alkali metals, such as Ca, Mg, Na and K, are however not available. These four cations and Si are naturally present in soil porewaters and solubility experiments where these constituents may form U(VI) bearing solids need to be performed to fully verify calculations such as we presented. Cement weathering products especially provide large quantities of Ca, Na, K and Si to the reacting waters and the formation of less soluble U(VI) bearing: 1) silicates, 2) Ca-silicates, and 3) alkaline earth uranates are very plausible. For conservative bounding calculations for near-neutral pH conditions, constraining the maximum concentrations of dissolved U(VI) by the solubility of the mineral schoepite remains a technically defensible approach. Only if more realistic calculations are required would one need to explore whether the other plausible U(VI) solids with lower solubilities are present.

The calculations showed that the mass of cement present in the streamtube (simulates the weathering waste-form within the shallow land burial ground) changes substantially with time. Additional computations to examine changes in porosity due to cement dissolution may be important to this study, because an increase in porosity will lead to a lower solid/water ratio and potentially to a quicker rate of cement dissolution. Future work should also include a sensitivity analysis of hydrodynamic dispersion on the concentrations of dissolved major elements and U(VI).

Acknowledgments

The authors wish to acknowledge the support of Westinghouse Hanford Company's Solid Waste Management Division for the funding to perform this work, especially Ken L. Hladek. We also wish to thank David Turner from Southwest Research Center, San Antonio, Texas for supplying us with his extended thermodynamic database including U minerals and aqueous species that was used to improve our existing MINTEQA2 data base. Finally we wish to thank Shas Mattigod (PNNL) for his technical review of this report and Suzette Burckhard (Kansas State University) for performing corroborative U solubility calculations using the MINTEQ computer code and her own conceptual model during her stay at PNNL in the summer of 1995.

Contents

Figures

Tables

1.0 Introduction

One proposed method of low-level radioactive waste (LLW) disposal is to mix the radioactive waste streams with cement, place the mixture in steel barrels, and dispose of the barrels in near-surface unsaturated sediments. Cement or concrete is frequently used in burial grounds, because cement porewaters are buffered at high pH values and lanthanides and actinides are very insoluble in highly alkaline environments. Therefore, leaching of these contaminants from the combined cement/low-level radioactive waste streams will at least initially be retarded. The calculations performed in this study demonstrate that the pH of cement porewaters will be maintained at a value greater than 10 for 10,000 years under Hanford specific hydrogeochemical conditions. Ten thousand years is the period generally studied in long-term performance assessments per regulatory guidance. The concentrations of dissolved hexavalent uranium [U(VI)], the valence form of dissolved U usually present in oxidizing surface and groundwaters, are also constrained by the high pH and predicted solution compositions over the 10,000-year period, which is favorable from a long-term performance perspective.

1.1 Cement Models

Due to the slow hydration process of cementitious material, there are problems in quantifying the chemical composition of cement porewater with predictive equilibrium models. The major problems are: 1) the hydrated reaction products in cement are solid solutions; and 2) the cement/porewater system is always in a transient, nonequilibrium state due to the slow diffusion of elements to the porewater from unreacted pockets of original cement minerals through hydrated alteration layers. Despite these problems, equilibrium models can be used to represent the dynamic chemical evolution of solids and porewaters by representing solid solutions as physical mixtures of pure end members and representing transient states as a progressive series of equilibrium states (Reardon 1992).

1.1.1 pH of Cement Porewater

The pH of porewater in cements evolves in several stages when the cement is in contact with water. Initially, the pH is controlled by KOH and NaOH leached from the cement. These compounds are totally soluble and will be removed on relatively short time scales. When controlled by these compounds, the pH of the cement porewater may exceed 13. Then, as leaching continues, the pH of the porewater is buffered at 12.5 by the solubility of the solid portlandite, $Ca(OH)_2$. Finally, the pH is controlled by the hydrated calcium silicates, which dominate the long-term behavior of the cement in the repository (Haworth et al. 1989). Because the KOH/NaOH and $Ca(OH)_2$ stages are finite and a high pH is maintained, investigators (e.g., Haworth et al. 1989; Gardiner et al. 1989) interested in the long-term behavior of a repository for radioactive waste frequently ignore these stages in cement/porewater evolution and focus on the dissolution of the hydrated calcium silicate gel (CSH-gel) that structurally holds the cement together.

1.1.2 Cement/Porewater Chemistry

Several simple models to describe the dissolution of CSH-gel have been developed. Solubility data on CSH-gel found in the literature are well represented by the solid solution model developed by Atkinson et al. (1987). They describe the aqueous solubility of CSH-gel by assuming that both SiO_2 (am, amorphous) and $Ca(OH)_2$ can form solid solutions with an intermediate compound having a

composition close to that of the mineral tobermorite [$Ca_5Si_6(O,OH)_{18}\cdot 5H_2O$, C/S = 0.833 where C is Ca and S is Si]. The Gibbs free energies of formation of the solid phases in the system are then described by the free energy of formation of the end members, the intermediate compound and solid solution interaction parameters. The choice of an intermediate compound similar to tobermorite is consistent with observations of a tobermorite-like structure within the CSH-gel.

Because most thermodynamic equilibrium codes do not include solid solution models, Berner (1988) developed a model that simulates the incongruent dissolution of CSH-gel by describing the gel as a mixture of congruently soluble components with variable solubility products. The main assumptions of Berner's model are: 1) the whole range of C/S ratios for the calcium silicates can be divided into three regions, and 2) within each region, the solid is considered to be a non-ideal mixture of congruently soluble components that each have a variable solubility product depending on C/S ratio. There are two C/S ratios where there is a sharp change in the solubility behavior and these form the boundaries between different regions. For the region below C/S = 1, the solid is described as a mixture of SiO_2 and CaH_2SiO_4, both with variable solubility products. Between C/S = 1 and C/S = 2.5, $Ca(OH)_2$ with a variable solubility product and CaH_2SiO_4 with a constant solubility product are assumed. For C/S > 2.5, $Ca(OH)_2$ and CaH_2SiO_4 are again used to describe the hydrated calcium silicates, but the associated solubility constants are held constant.

Haworth et al. (1989) incorporated Berner's model for the incongruent dissolution of cement into a coupled reaction/transport model in order to predict the long-term buffering capacity of the cement. Gardiner et al. (1989) and Alcorn et al. (1989, 1990) chose to describe cement grout as a mixture of three minerals: 14-Å tobermorite ($Ca_5Si_6O_{17}\cdot 10.5H_2O$), hydrogarnet ($Ca_3Al_2O_6\cdot 6H_2O$), and ettringite [$Ca_3Al_2(CaSO_4)_3\cdot 32H_2O$] in order to perform calculations to predict the life-span of grout seals for a repository. In their models, 14-Å tobermorite was used as a substitute for the CSH-gel. Criscenti and Serne (1990) determined the hydrated mineral assemblage for Portland Type III cement using Berner's (1987) cement hydration model. The mineral afwillite ($3CaO\cdot 2SiO_2\cdot 3H_2O$) was used as a substitute for CSH-gel in subsequent calculations to predict leachate compositions from cement waste forms. Afwillite is stoichiometrically similar to CSH-gel and is the end product of the hydration of pure tricalcium silicate.

Glasser et al. (1988) developed a model to predict the equilibrium phase distribution in slag-cement blends. His model for the $CaO\text{-}Al_2O_3\text{-}SiO_2\text{-}MgO\text{-}H_2O$ system consists of the following solid phases: portlandite [$Ca(OH)_2$], gehlenite hydrate ($2CaO\cdot Al_2O_3\cdot SiO_2\cdot 8H_2O$), hydrotalcite [$6MgO\cdot Al_2O_3\cdot (OH)_x\cdot yH_2O$], monosulfate ($4CaO\cdot Al_2O_3\cdot SO_3\cdot 12H_2O$), and poorly crystalline CSH-gel. Glasser et al. (1988) did not address the issue of how to characterize the CSH-gel for incorporation into predictive computer codes.

Reardon (1992) emphasized that the principal cations in fresh cement porewaters are Na^+ and K^+, and that the concentrations of these cations will dictate the solution pH. The alkalis are present as soluble sulfates that dissolve early in the cement hydration process and as minor constituents in solid solution with the dry, unreacted cement "clinker" minerals. Reardon (1992) suggested that, without Na^+ and K^+, the porewater will be in equilibrium with $Ca(OH)_2$, CSH-gel, hydrogarnet, brucite, and either ettringite or monosulfate. The concentrations of Ca, Mg, Al, Si, and SO_4 will be independent of water/cement ratio, hydration kinetics, extent of hydration, and cement composition. On the other hand, the alkali concentrations will be a function of the cement mix and the hydration process.

Reardon (1992) attempted to describe the hydration of cement using a thermodynamic ion-interaction model. Studies on the longevity of cement for repository environments (e.g., Haworth et al. 1989) start with the premise that the cement is completely hydrated and that the alkalis have already been flushed out of the porewater through the interaction with the environment. This assumption is adequate only if the effects of high ionic strength solutions on the solubility of radionuclides can be ignored, an assumption we feel has merit.

1.1.3 Actinide and Lanthanide Solubilities in Cement Porewater

The insolubility of actinides and lanthanides at high pH conditions in low ionic strength solutions is well documented. However, during the earliest stage of cement leaching, the ionic strength of the porewater is high. To describe the cement behavior and examine the effect of ionic strength on mass transfer between the solid and porewater during the earliest stage, calculations with a thermodynamic Pitzer ion-interaction model (Pitzer 1991) are likely necessary.

Studies to determine the behavior of actinides and lanthanides in solutions characterized by both high pH values and high ionic strengths have only recently been initiated. Preliminary results, with ion-interaction parameters, are described, for example, in studies by Felmy et al. (1989, 1990, 1991, 1993), Felmy and Rai (1992), Rai et al. (1992), and Roy et al. (1992). From these studies, we conclude that, for trivalent and tetravalent actinides only, high concentrations of F^- or CO_3^{2-} ligands would increase the solubility. It is unlikely that cement environments would allow high concentrations of these ligands, because the Ca present will combine with these ligands to precipitate fluorite and calcite. Thus high ionic strength corrections may not be necessary for the prediction of actinide and lanthanide solubilities under conditions where actinides and lanthanides are present in the III and IV valence states and the ionic strengths are limited by the formation of CaF_2 and $CaCO_3$ solids. In general, ligand interactions, excepting U(VI)-carbonate, with U(V) and U(VI) valence states are weaker than for U(III) and U(IV). Therefore, high ionic constructs, such as the Pitzer ion-interaction model (Pitzer 1991) are not necessary to accurately perform the U(VI) solubility calculations described in Chapter 4. That is, activity corrections using the extended Debye-Hückel equation, such as that in the MINTEQA2 computer code (Allison et al. 1991), should yield realistic predictions for cement/porewater reactions.

1.2 Cement/Water Modeling for Repository Environments

The research of Haworth et al. (1989, 1990) was sparked by interest in the United Kingdom (UK) in using a cementitious backfill as an engineered barrier in its design for low- and intermediate-level nuclear waste repositories. The high pH environment introduced by the cementitious backfill will reduce the general corrosion rate of metal canisters and radionuclide mobility.

Haworth et al. (1989, 1990) incorporated Berner's (1988) model for CSH-gel dissolution into the CHEQMATE computer code. The CHEQMATE code is a coupled chemistry/transport model that uses the PHREEQE geochemical reaction code (Parkhurst et al. 1980) to calculate aqueous speciation and solubility. The transport part of the code includes diffusion, advection, and electromigration. Within CHEQMATE, transport is solved for one-dimension by a finite difference method.

Haworth et al. (1989) performed diffusion-only calculations, in which cement leached into pure water. In a following paper, Haworth et al. (1990) compared the advection of demineralized water

and groundwater through cements of various compositions. Calculations and experiments showed that interaction with groundwater will lead to a quicker decrease in cement porewater pH than interaction with demineralized water. After 100,000 years, the pH at the center of an 11-meter block of cement dropped below 10 for the cement in contact with groundwater, but was still predicted to exceed 11 for the cement in contact with demineralized water. Haworth et al. (1990) also concluded that cements with low C/S ratios were not suitable for maintaining a high pH in the near-field of a repository.

1.3 Coupled Reaction/Transport Model (CTM)

The CTM (Contaminant Transport Model) computer code, developed at PNNL (Schramke et al. 1992), is a coupled reaction/transport model that can simulate transport and reaction of aqueous solutions in porous, homogeneous media along a one-dimensional streamtube under steady-state flow conditions. The CTM code uses a two-step algorithm to link the hydrologic and geochemical modules that perform the calculations. The geochemical module can be used to calculate aqueous complexation, the precipitation and dissolution of solid phases, and the adsorption and desorption of aqueous species to solid surfaces. The distribution of components between aqueous species is determined using a modified Newton-Raphson technique. A Markov approach is used to solve the advection/dispersion transport equation.

Input for CTM consists of a geochemical model, a hydrologic model, initial conditions and boundary conditions. The code can be run with 1) no geochemistry; 2) equilibrium speciation, solubility, and adsorption; or 3) constant K_d adsorption. If the full geochemistry option is selected, then the user must enter the chemical components, solids, adsorbates, adsorbents, and aqueous species that will be considered for the geochemical model. Therefore, it is important to completely define the geochemical conceptual model prior to using CTM. For example, it can be important for a cement system to review which solid phases might precipitate as the hydrated cement phases dissolve and how the pH of the porewater changes through time.

Input for the hydrologic model includes the number of bins, the length of the streamtube, the time increment, the porewater velocity, and the dispersion coefficient. A probability density function is used to describe advection and dispersion in the streamtube. Values for the Peclet number, Courant number, and row sum are calculated. This output is used to adjust the number of bins and time increments to reduce numerical dispersion in the calculations and assure that mass balance is maintained in the streamtube.

The initial conditions are defined by the initial aqueous concentrations (molal) of the components, the initial concentrations (mol/kg H_2O) of solids (including adsorbents) in the streamtube, and the initial concentrations (mol/kg H_2O) of the adsorbates bound to adsorbents in the streamtube. The boundary conditions are defined by the influent composition through time for the calculation.

In order to perform calculations involving cement dissolution, Berner's (1988, 1990) incongruent dissolution model was incorporated into CTM. After the mass of each component has been redistributed by the transport module, each bin is reequilibrated. Prior to each calculation of the equilibrium assemblage in a bin, the moles of calcium and silicon in the solid phases [$Ca(OH)_2$, SiO_2 (am), and CaH_2SiO_4] used to define CSH-gel are summed and the C/S ratio determined. New equilibrium constants, using Berner's (1988,1990) empirical equations are defined. These equations are provided in Table 1.1.

Table 1.1. Simplified Chemical System Used to Model the Incongruent Dissolution of Hydrated Calcium Silicates Based on Berner (1990)

Region	C/S Range	Model Components	Apparent Solubility Product of Model Components as a Function of C/S
	C/S = 0	SiO_2	$\log K_{sp} = -2.71$
I	$0 < C/S \leq 1$	SiO_2	$\log K_{sp} = -1.994 + [0.861 / (C/S - 1.2)]$
		CaH_2SiO_4	$\log K_{sp} = -7.12 - [(1 - C/S) / (C/S)] \times \{0.79 + [0.861 / (C/S - 1.2)]\}$
II	$1 < C/S \leq 2.5$	$Ca(OH)_2$	$\log K_{sp} = -4.945 - [0.338 / (C/S - 0.85)]$
		CaH_2SiO_4	$\log K_{sp} = -7.12$
III	$C/S > 2.5$	$Ca(OH)_2$	$\log K_{sp} = -5.15$
		CaH_2SiO_4	$\log K_{sp} = -7.12$

1.4 Geochemical Reaction Model (MINTEQA2)

Modeling of concentration limits for dissolved U(VI) based on solubilities of U-bearing solids was completed separately from the pH evolution calculations that used the CTM code. The large number of possible U(VI) aqueous species and solids that should be considered in performing comprehensive U(VI) solubility calculations would be difficult to include in the CTM code and would result in very long computation run times. Moreover, at the time this work was performed, the main author (L. J. Criscenti) was on an off-site assignment and had access to limited computing facilities.

The U(VI) solubilities and associated aqueous speciation equilibria were calculated using the personal computer (PC) version of the chemical equilibria code MINTEQA2 (Version 3.10).[a] The MINTEQA2 code and its predecessor versions have been described by Felmy et al. (1984, MINTEQ), Peterson et al. (1987, MINTEQ), Brown and Allison (1987, MINTEQA1), and Allison et al. (1991, MINTEQA2). The code was originally constructed by combining the mathematical structure of the MINEQL code (Westall et al. 1976) with the thermodynamic database and geochemical attributes of the WATEQ3 code (Ball et al. 1981). The MINTEQ calculations may include aqueous speciation, solubility and saturation state (i.e., saturation index), adsorption, oxidation-reduction, gas phase equilibria, and precipitation/dissolution of solid phases. The MINTEQ code incorporates a Newton-Raphson iteration scheme to solve the set of mass-action and mass-balance expressions, and uses the Davies and extended Debye-Hückel equations to calculate activity

(a) The PC version of the MINTEQA2 code was obtained from the Center for Exposure Assessment Modeling at the U.S. Environmental Protection Agency (EPA) in Athens, Georgia.

coefficients for aqueous ions. The reader is referred to the references and user guides listed above for details regarding the use of MINTEQ code, types and examples of geochemical equilibria calculations possible with this code, and the basic equations on which the model is based.

The MINTEQ code is used in conjunction with a thermodynamic database to calculate complex chemical equilibria among aqueous species and solubility constraints. The thermodynamic data used to calculate U(VI) solubilities include the database originally supplied with the MINTEQA2 code by the U.S. Environmental Protection Agency (EPA) and the addition of U-bearing species, solids, and associated thermodynamic data primarily from Grenthe et al. (1992) and several secondary sources. The complete MINTEQA2 thermodynamic database for U-bearing aqueous species and solids and the sources used for these data are listed in the appendix.

Output from the CTM code was used as part of the input for the MINTEQA2 calculations of solubility limits for dissolved U(VI). The required output from CTM included the chemical composition of the equilibrium water leaving each bin at specific travel times. For each specific water composition, the MINTEQA2 calculates the distribution of aqueous species involving all dissolved chemical components. The MINTEQA2 code then recalculates the final equilibrium composition of each water using any solubility constraints applied by the user to the geochemical system. For a subset of the scenarios considered in this study, the solubility of U(VI) was calculated by assessing the total amount of U(VI) that would be in equilibrium with one of three likely U-bearing solid phases. These solids included schoepite ($UO_3 \cdot 2H_2O$), uranophane [$Ca(UO_2)_2(SiO_3)_2(OH)_2 \cdot 5H_2O$)], or calcium uranate ($CaUO_4$). These three U-bearing solids were chosen as possible solubility-limiting phases based on results from published studies that suggest these solids have commonly been found to form in low temperature aqueous environments typical of the shallow land burial ground environments (both natural and cement influenced).

2.0 Conceptual Models and Input Data

This chapter details the conceptual models used to predict the evolution of the pH and compositions of the cement porewater, and calculate the solubility-limited concentrations of dissolved U(VI).

2.1 Waste Disposal Scenarios

To evaluate the potential for suppressing the release of U, specifically U(VI), from low-level radioactive (LLW) waste solidified in cement for 10,000 years at the Hanford Site, sixteen waste disposal scenarios were evaluated. These scenarios are described by the permutations of two choices for each of four variables: the recharge rate, the composition of the influent solution, the length (or number) of waste drums in the flow path, and the mass of cement per waste drum. From sixteen potential disposal scenarios, coupled reaction/transport calculations were performed for nine of the scenarios. Results for the other seven scenarios are deduced from these calculations. The sixteen potential scenarios are described in Table 2.1 and the scenarios for which calculations were performed are indicated in the far right column of Table 2.1. Input parameter selection for these scenarios is described below.

2.2 LLW Source Term

The dimensions of the barrels used to contain the low-level radioactive waste mixed with cement are assumed to be 59.8 cm in diameter and 88 cm in height, which are equivalent to the dimensions given in catalogs for 55-gal drums. The barrels are assumed to be made of Fe metal (steel) that is approximately 0.127 cm thick as designated in supply catalogs. The Fe barrels have a lifetime in Hanford soil of 20 to 200 years.[a] Because of the short lifetime of the barrel, the effects of Fe-metal degradation on the cement porewater composition and surrounding soil water are not considered in the calculations presented.

Changes in cement porewater and effluent compositions [especially for U(VI)] are modeled as a function of time for two barrel configurations: 1) one barrel of cement, and 2) three barrels that are stacked on top of each other. The latter is a plausible design for the waste disposal site. For this study, the total height taken up by the stacking of each barrel is assumed for convenience to be 1 m (an approximate round off of the 88 cm barrel height). The flow path consists of recharge water or porewater percolating from the site surface, vertically through the burial ground and into the underlying vadose zone sediments. The modeling simulations are therefore completed for lengths of 1 m (i.e., one barrel) and 3 m (i.e., three barrels) of cement-containing waste.

Each barrel will contain a mixture of cement and waste. Calculations are performed assuming that 1) each barrel is completely filled with cement (that contains excess U), or 2) each barrel is a homogeneous mixture of one third cement and two thirds inert waste material that contains excess U. These options are intended to provide the maximum and minimum mass of cement that will be found in any flow path through the disposal site if wastes are solidified in cement.

(a) L. Roy Bunnell, Pacific Northwest National Laboratory (PNNL), personal communication.

Table 2.1. Sixteen Scenarios Considered for Coupled Reaction/Transport Modeling Using Four Variables

Scenario	Recharge Rate (cm/yr)	Influent	Length of Cement Column (m)	Barrel Contents	CTM Model Run #
A	0.5	Rain Water	1	Cement	7,8
B	0.5	Rain Water	1	1/3 Cement 2/3 Waste	9,10
C	0.5	Soil Porewater	1	Cement	31
D	0.5	Soil Porewater	1	1/3 Cement 2/3 Waste	30
E	0.5	Rain Water	3	Cement	None
F	0.5	Rain Water	3	1/3 Cement 2/3 Waste	None
G	0.5	Soil Porewater	3	Cement	None
H	0.5	Soil Porewater	3	1/3 Cement 2/3 Waste	None
I	5	Rain Water	1	Cement	None
J	5	Rain Water	1	1/3 Cement 2/3 Waste	23
K	5	Soil Porewater	1	Cement	None
L	5	Soil Porewater	1	1/3 Cement 2/3 Waste	None
M	5	Rain Water	3	Cement	24
N	5	Rain Water	3	1/3 Cement 2/3 Waste	22
O	5	Soil Porewater	3	Cement	29
P	5	Soil Porewater	3	1/3 Cement 2/3 Waste	28

2.3 Composition of Cement/Grout

The cement/grout mixture for the disposal of low level radioactive waste has not been selected for the disposal site. For the sixteen scenarios, Portland Cement Type I, also called Ordinary Portland Cement (OPC), is used. The composition for this cement is given in Table 2.2. The C/S ratio (2.7) for this cement is determined by the moles of Ca and Si present in the dry calcium silicates (C_3S and

C_2S, where $C_3S = 3CaO \cdot SiO_2$ and $C_2S = 2CaO \cdot SiO_2$). The hydrated phases in Berner's cement model for a C/S ratio of 2.7 are $Ca(OH)_2$ and CaH_2SiO_4. The dry calcium silicates are reacted with water to form these phases.

Table 2.2. Composition of Portland Cement Type I

Oxide Basis	Weight %	Compound Basis[a]	Weight %
CaO	63.8	Free C	0.4
MgO	3.7	C_4AF	7
Al_2O_3	5.6	C_3A	11
Fe_2O_3	2.4	C_3S	55
SiO_2	20.7	C_2S	18
TiO_2	0.23		
Na_2O	0.21		
K_2O	0.51		
SO_3	1.6		

(a) C = CaO, A = Al_2O_3, F = Fe_2O_3, S = SiO_2

In Berner's incongruent dissolution model, the CSH-gel is represented by three components: portlandite [$Ca(OH)_2$], CaH_2SiO_4, and SiO_2 (am). Simple calculations were performed with GM (Geochemical Model) computer code, an aqueous speciation/solubility submodel of CTM, to simulate the equilibration of distilled water with each of these components. The calculated pH values for these solutions are 12.5 with respect to equilibrium with $Ca(OH)_2$, 10.9 with respect to equilibrium with CaH_2SiO_4, and 6.3 with respect to equilibrium with SiO_2 (am). These calculations suggest that cements with a high C/S ratio will sustain high pH environments longer than cements with a low C/S ratio. This hypothesis is consistent with experimental observations by Haworth et al. (1990).

During the model simulations, the composition of the cement was allowed to change according to Berner's incongruent dissolution model. In addition, the precipitation of calcite ($CaCO_3$), brucite [$Mg(OH)_2$], and gypsum ($CaSO_4 \cdot H_2O$), is permitted in the simulations if the solutions become oversaturated with these solids. Because a fluorine concentration is included in the analysis of the Trench 8 porewater, precipitation of fluorite (CaF_2) was also allowed in simulations using this influent.

2.4 Recharge Rates

The estimated recharge rates for the Hanford Site provided by staff from Westinghouse Hanford Company are 5.0 and 0.5 cm/yr. The porosity of cement ranges from 0.20 to 0.30 (Lea 1988). For the calculations in this report, a cement porosity of 0.20 was selected and the cement was assumed to be fully saturated. The porewater velocity was defined as the recharge rate divided by the volumetric water content for the fully saturated cement. Therefore, porewater velocities of 2.5 and 25 cm/yr are derived from the values of the parameters given. A porewater velocity of 2.5 cm/yr is reasonable through cement; a velocity of 25 cm/yr is high for water passing through a cement block and should lead to a conservative estimate of cement longevity. For the porewater velocities of 2.5 and 25 cm/yr, dispersion coefficients of 0.0001 and 0.001 m^2/yr, respectively, are used. Through these selections, the ratio of advection to dispersion is constant for all calculations.

2.5 Compositions of Influent Solutions

The compositions of influent solutions selected include those for a rainwater and Hanford soil saturation extract. These solutions are intended to bound the compositions of aqueous solutions that might contact the cement in the low-level radioactive waste burial ground. Given a high recharge rate, the rainwater may not have time to equilibrate with the soil before reacting with the cement. Given a low recharge rate, the soil porewater may reach equilibrium with the soil and contain a higher concentration of total dissolved solids.

The rainwater composition used in this study (Table 2.3) is the average rainwater composition for Menlo Park, California during the winters of 1957-1958. The rainwater composition was selected from the literature, because a documented report of the composition of rainwater at the Hanford Site was not found. The selected rainwater composition is given in Table 7.1 of Freeze and Cherry (1979) along with six other rain and snow compositions. For these seven analyses listed in Freeze and Cherry, the rainwater pH varies from 4.1 to 5.9 and bicarbonate concentration varies from 1.95 to 3.0 mg/L.

The composition of soil solution used in this study (Table 2.3) is porewater from Trench 8 (Serne et al. 1993, Table 9) at the Hanford Site. Results of a geochemical speciation/solubility calculation indicated that the reported composition for this soil solution was slightly out of charge balance and oversaturated with respect to calcite. The composition used in the CTM calculations was therefore modified by the subtraction of some Cl and equilibrated with calcite. The solution composition was charge balanced by decreasing the concentration of Cl which was decreased from 109 mg/L to 70.9 mg/L. Equilibration with calcite decreased the reported Ca and CO_3 concentrations by 0.22 mg/L and 0.35 mg/L respectively, which are relatively insignificant changes.

2.6 Streamtube

The cement was represented in the streamtube by CSH-gel consisting of the hydrated phases in Berner's model. The initial condition for each scenario consisted of a homogeneous streamtube containing the appropriate ratio and amounts of two cement phases $Ca(OH)_2$ and CaH_2SiO_4. They were chosen to proxy for OPC, and porewater in equilibrium with these phases at a pH of 12.5.

For a recharge rate of 0.5 cm/yr (porewater velocity of 0.025 m/yr), the CTM simulations were completed for 1 m of cement. The streamtube was divided into 5 bins, each 0.2 m in length. A time-step of 10 years was used.

For the faster recharge rate of 5.0 cm/yr (porewater velocity of 0.25 m/yr), the calculations were performed for 3 m of cement. For the 3-m streamtube simulations, the streamtube was divided into 15 bins, each 0.2 m in length. A time-step of 2 years was used, and 5000 time-steps were calculated per model simulation.

Table 2.3. Composition of Rainwater and Soil Porewater

Component	Rain Water	Soil Porewater
pH	5.9	7.87
	----------(mg/L)----------	
H_4SiO_4	0.46	63.6
Ca	0.77	58.28[a]
Mg	0.43	15.0
Na	2.24	34.8
K	0.35	6.8
CO_3	1.92	77.65[a]
SO_4	1.76	85.0
Cl	3.75	70.9[a]
NO_3	0.15	<0.5
F	NA[b]	1.00

(a) The concentrations of Ca, CO_3, and Cl listed for Trench 8 porewater in Serne et al. (1993) were modified for the CTM calculations by assuming equilibrium with the solubility of calcite and increasing the Cl concentration to charge balance the solution composition.
(b) NA ≡ concentration not available.

3.0 Results of Coupled Reaction/Transport Calculations

Coupled reaction/transport was calculated using CTM for Scenarios A through D, Scenario J, and Scenarios M through P (see Table 2.1). The predicted changes in cement and porewater chemistry are described below in detail as a function of time for Scenarios A, B, and D.

The CTM simulations for Scenarios C, J, M, N, O, and P are not discussed in detail, because the evolution of their pH and chemical systems through the first 10,000 years is not significantly different than one of the three scenarios discussed in detail below. In many scenarios, very few changes occur during the first 10,000 years, and excess $Ca(OH)_2$ component in the cement keeps the porewater pH ($\approx$ 12.5) and composition fairly constant. In general, evolution of the porewater pH and system chemistry predicted by CTM for Scenarios J and N resemble those for Scenario B with only the event times being different. The same is true for the pairs of Scenarios A and M, D and P, and C and O. Scenario V, and thus O, show an evolution pattern for pH and system chemistry that is quite similar to that for Scenario D excepting that the times for significant decreases in porewater pH are later because three times more cement is present.

3.1 Scenario A

Figures 3.1a, 3.1b, and 3.1c illustrate the mass of the $Ca(OH)_2$, CaH_2SiO_4 and SiO_2 (am) end-member components, respectively, remaining in the CSH-gel in each bin (0.2 m long) as a function of time for Scenario A. As time increases, interaction between the cement and rainwater decreases the mass of $Ca(OH)_2$ present in each bin. As the $Ca(OH)_2$ end member of the CSH-gel dissolves, the C/S ratio of the gel decreases. When $Ca(OH)_2$ has disappeared from the system, SiO_2 (am) precipitates. The intermediate solid, CaH_2SiO_4, is present throughout the 10,000-year calculation. A maximum in the mass of CaH_2SiO_4 present in a bin occurs immediately prior to the onset of the precipitation of SiO_2 (am).

The calculated concentrations of dissolved Ca and Si in the porewater within each bin as a function of time for Scenario A are given in Figures 3.2a and 3.2b, respectively. Figure 3.2c illustrates the changes in pH as a function of distance and time. The Ca solution concentration is controlled by the masses of CaH_2SiO_4 and $Ca(OH)_2$ present in each bin. The concentration of dissolved Si is controlled by the masses of CaH_2SiO_4 and SiO_2 (am) in each bin. Both Ca and Si are maintained at lower solution concentrations when controlled by the solubility of CaH_2SiO_4 than when controlled by the solubility of $Ca(OH)_2$ or SiO_2 (am), respectively. Therefore, the higher the ratio of CaH_2SiO_4 to either $Ca(OH)_2$ or SiO_2 (am), the lower the Ca and Si concentrations in solution. The mass of CaH_2SiO_4 present buffers the pH of the cement porewater such that it does not decrease below 11.0 throughout the simulation.

Figures 3.3a and 3.3b illustrate the mass of precipitated calcite and the concentration of dissolved carbonate (CO_3) in the porewater, respectively, as a function of distance and time. The mass of precipitated calcite in each bin (distance) is small compared to the mass of the CSH-gel present throughout time (see Figure 3.1b). This suggests that the precipitation of solids will not have a major effect on the cement porosity for this scenario.

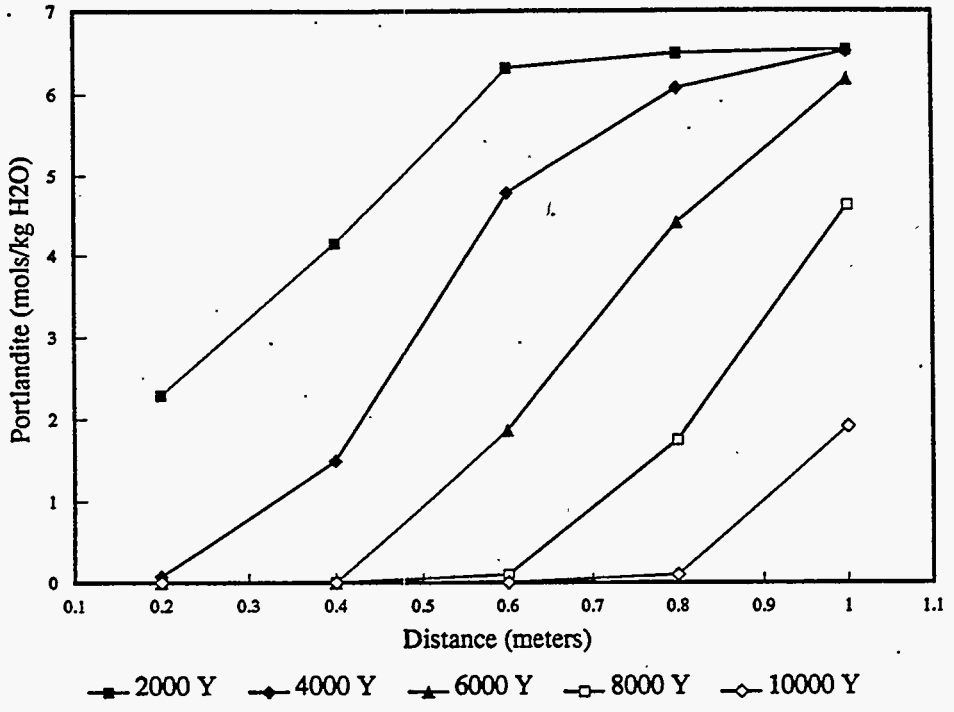

Figure 3.1a. Scenario A - Mass of $Ca(OH)_2$ Component in CSH-gel as a Function of Distance and Time

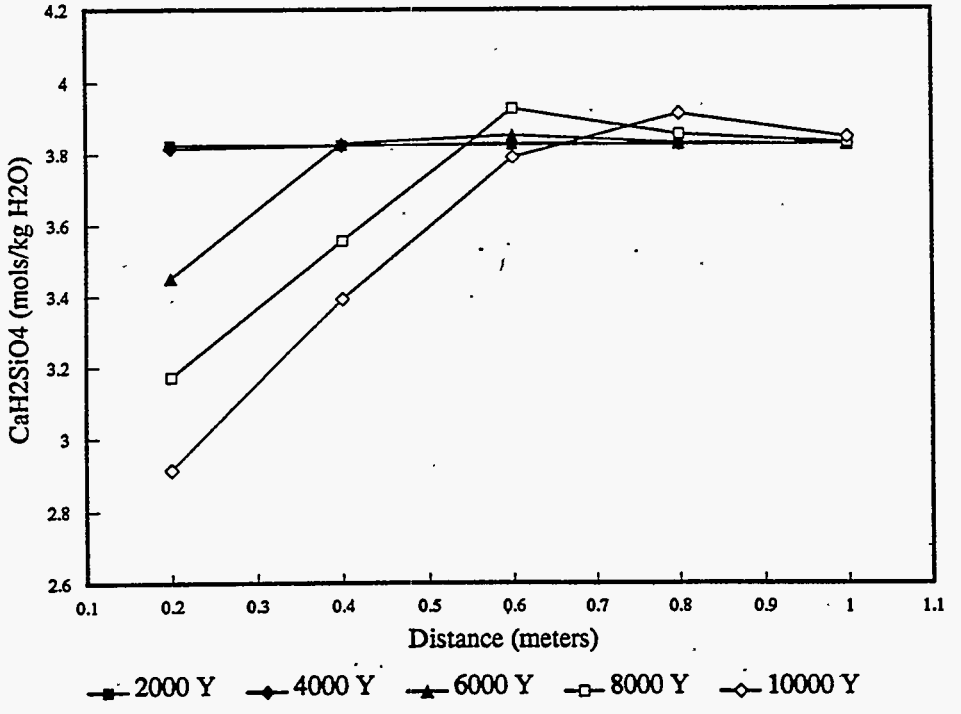

Figure 3.1b. Scenario A - Mass of CaH_2SiO_4 Component in CSH-gel as a Function of Distance and Time

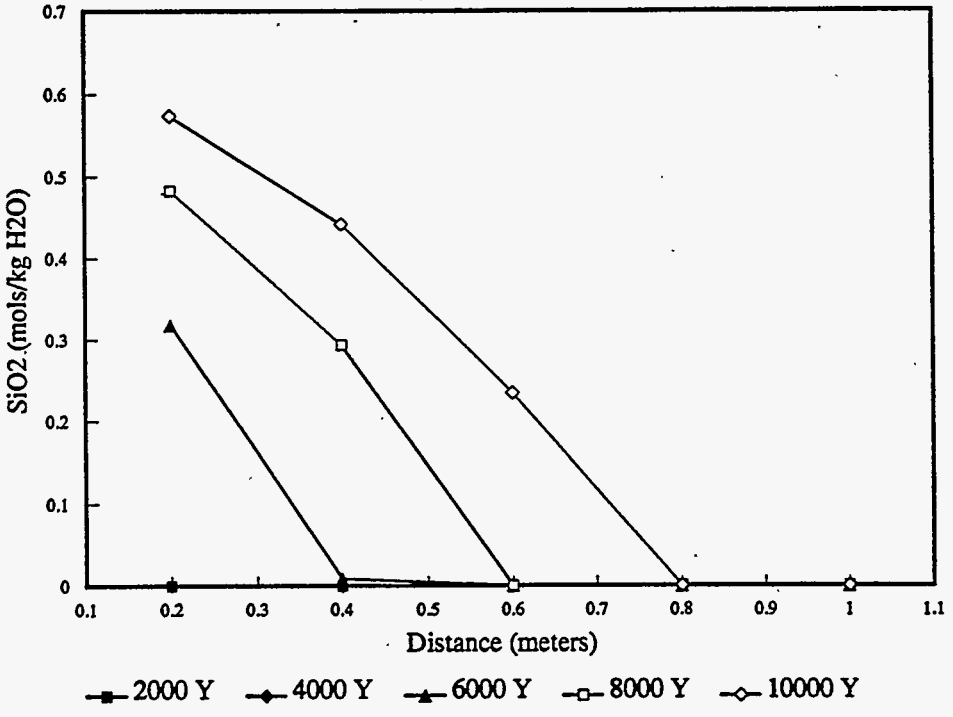

Figure 3.1c. Scenario A - Mass of SiO_2 (am) Component in CSH-gel as a Function of Distance and Time

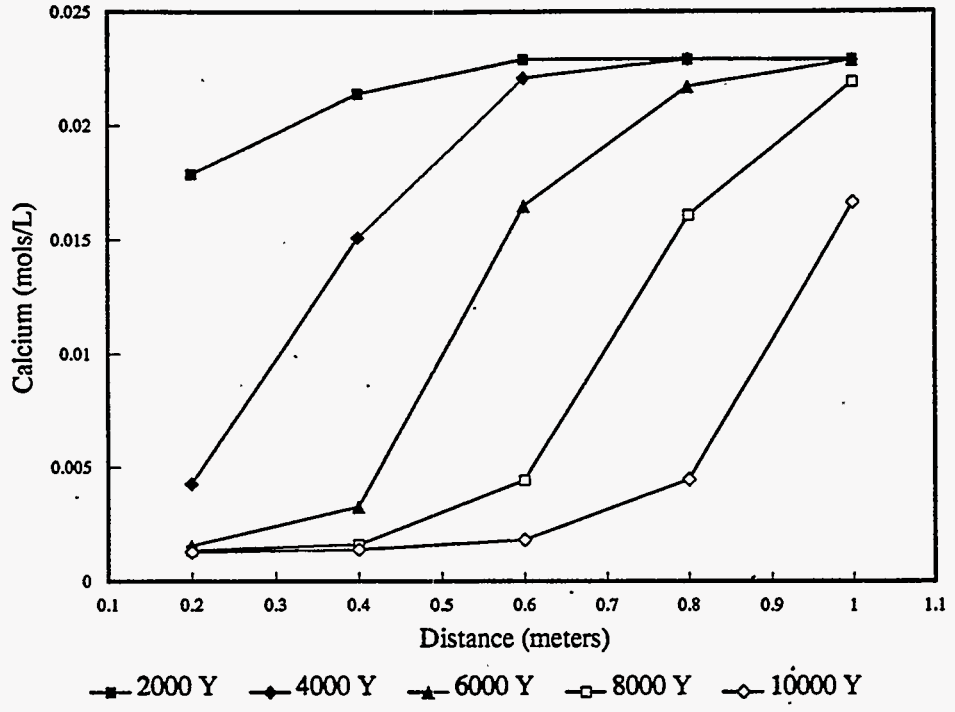

Figure 3.2a. Scenario A - Concentration of Dissolved Calcium in Porewater as a Function of Distance and Time

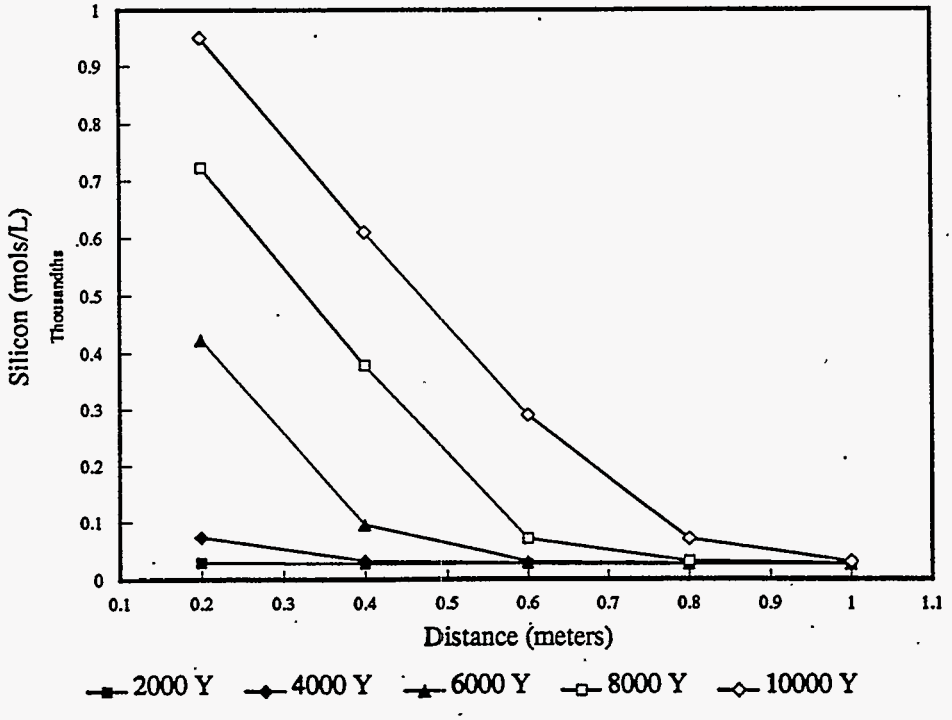

Figure 3.2b. Scenario A - Concentration of Dissolved Silicon (as Si) in Porewater as a Function of Distance and Time

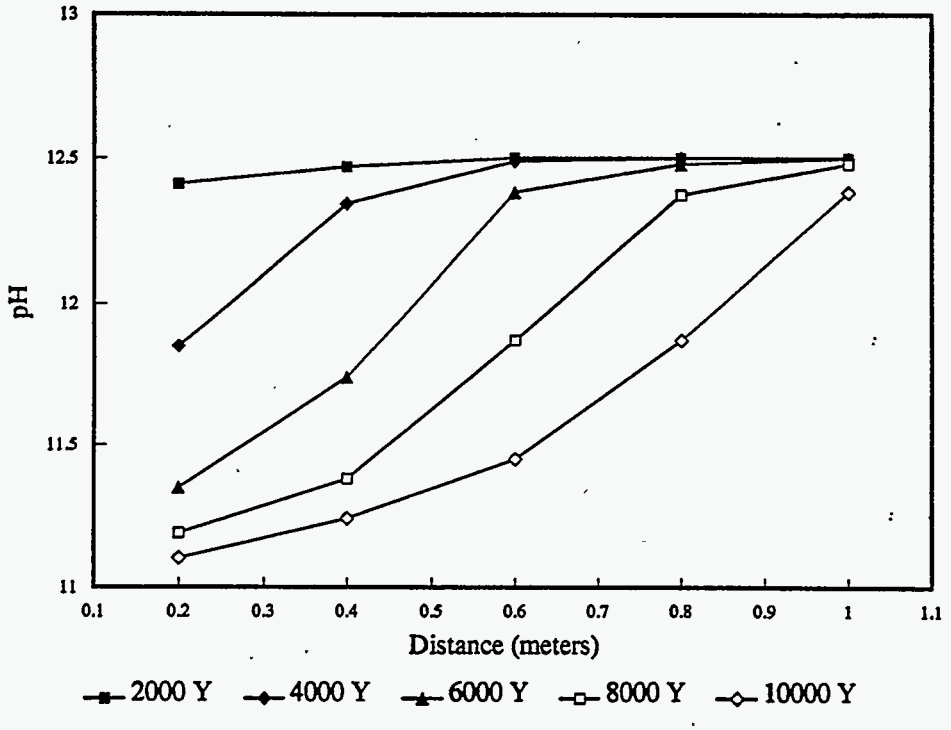

Figure 3.2c. Scenario A - pH of Porewater as a Function of Distance and Time

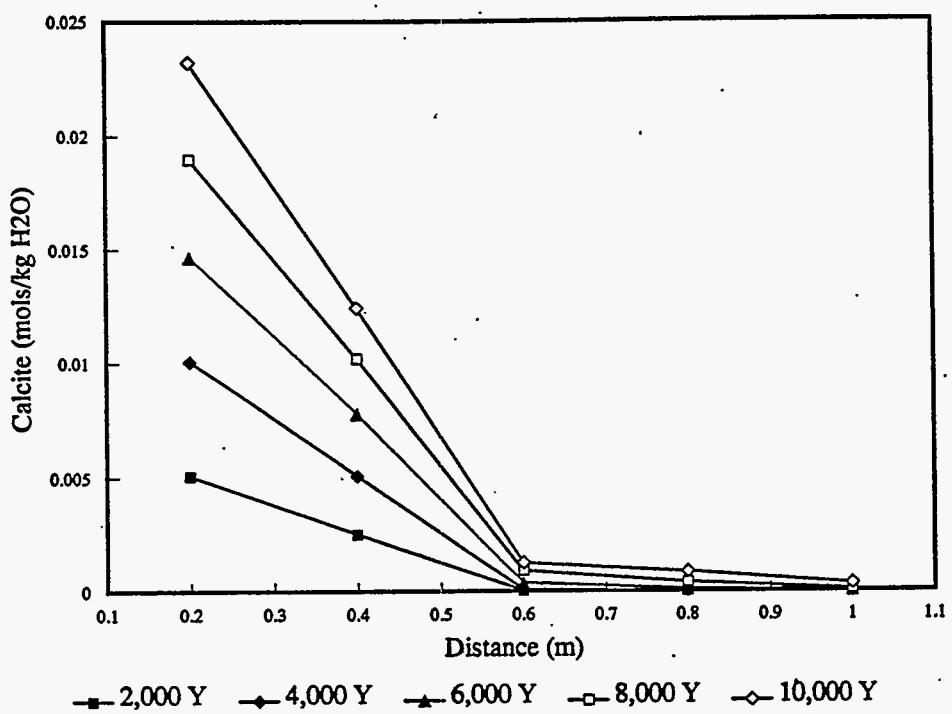

Figure 3.3a. Scenario A - Mass of Precipitated Calcite as a Function of Distance and Time

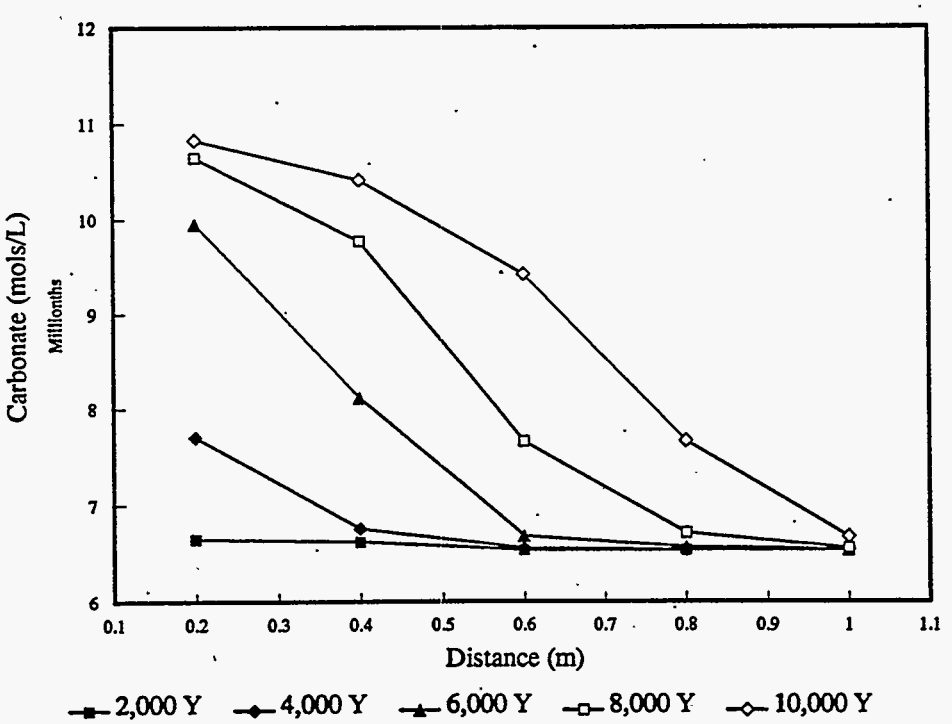

Figure 3.3b. Scenario A - Concentration of Dissolved Carbonate (CO_3) as a Function of Distance and Time

3.2 Scenario B

The mass of cement used as the initial condition for the Scenario B simulation is one-third the mass of cement used in Scenario A. The smaller mass of cement increases the rate of change in the cement-water system. Nonetheless, the pH of the cement porewater remains relatively high (pH > 10.5) over a 10,000-year period (Figure 3.4).

Figures 3.5a through 3.5e illustrate the mass of cement and the cement components in each bin at several times during the calculation for Scenario B. These diagrams show that the moles of cement present in the streamtube decrease with increased cement leaching. They also illustrate the changing ratios of the cement solids/reaction products $Ca(OH)_2$, CaH_2SiO_4, and SiO_2 (am) as a function of time. First, the ratio of $Ca(OH)_2$ to CaH_2SiO_4 decreases. Then, at approximately a pH of 11.5, $Ca(OH)_2$ disappears and the SiO_2 (am) end member of cement begins to precipitate. Finally, the ratio of SiO_2 (am) to CaH_2SiO_4 present increases.

Calcium, magnesium, silica (as H_4SiO_4), and carbonate solution concentrations for Scenario B are illustrated in Figures 3.6a through 3.6d. Brucite and calcite were predicted to precipitate, whereas the solution remains undersaturated with respect to gypsum throughout the calculation sequence. Figures 3.7a through 3.7e illustrate the moles of precipitated brucite and calcite as a function of time in bins 1 through 5. Again, the moles of precipitated solids are small compared to the initial moles of cement present in the streamtube. Less than 1% as many moles of brucite and calcite form compared to the moles of CaH_2SiO_4, and SiO_2 (am) present throughout the time period modeled. The dissolution of cement phases will affect cement porosity more than the precipitation of alteration products.

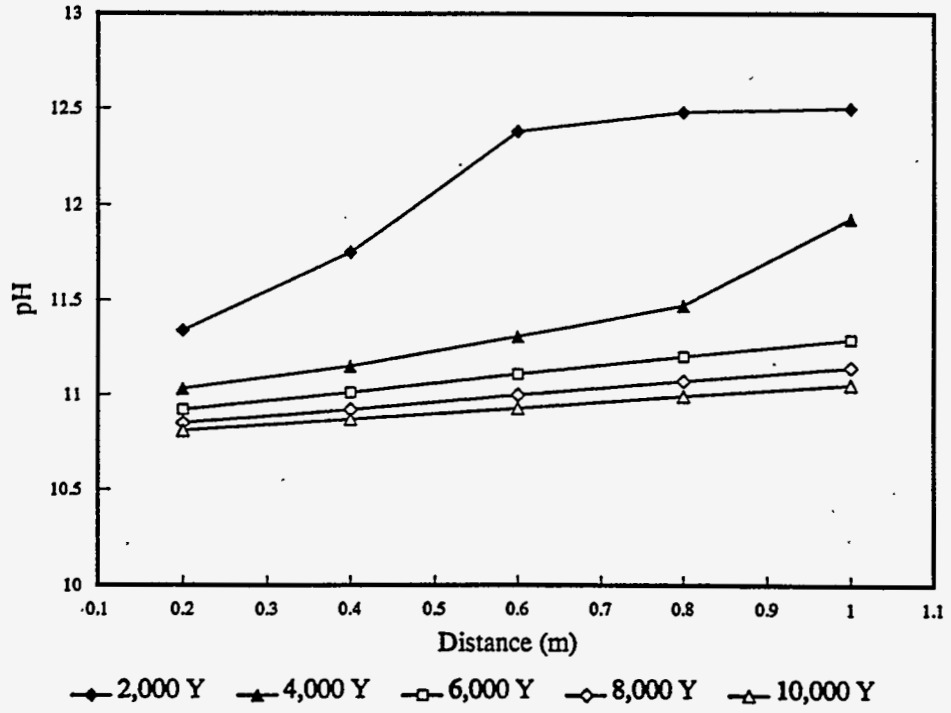

Figure 3.4. Scenario B - pH of Pore Water as a Function of Distance and Time

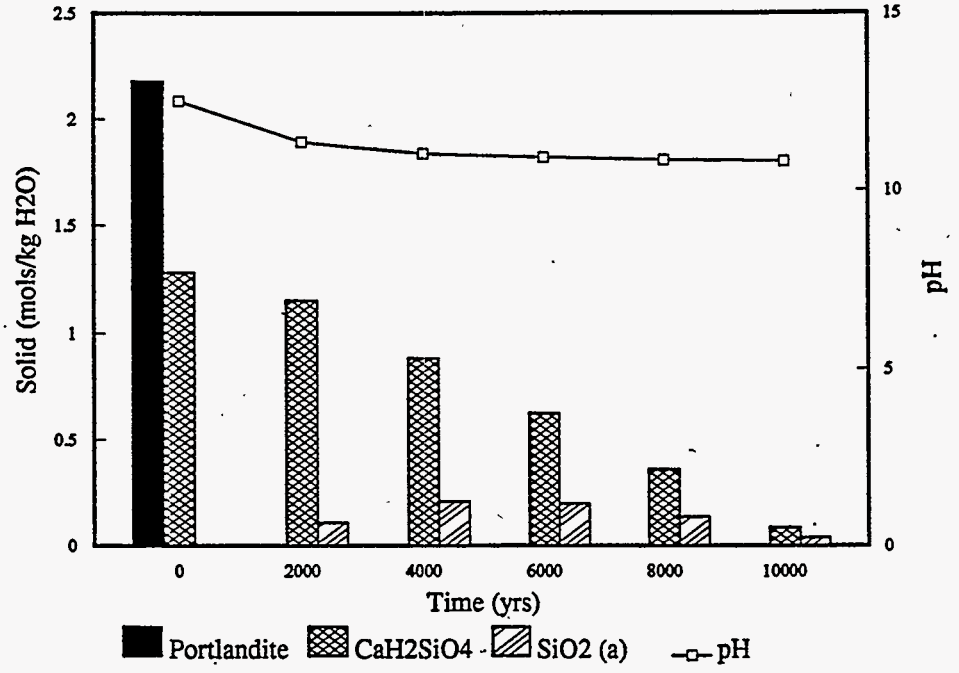

Figure 3.5a. Scenario B - Moles of Cement Present in Bin 1 (Distance) as a Function of Time

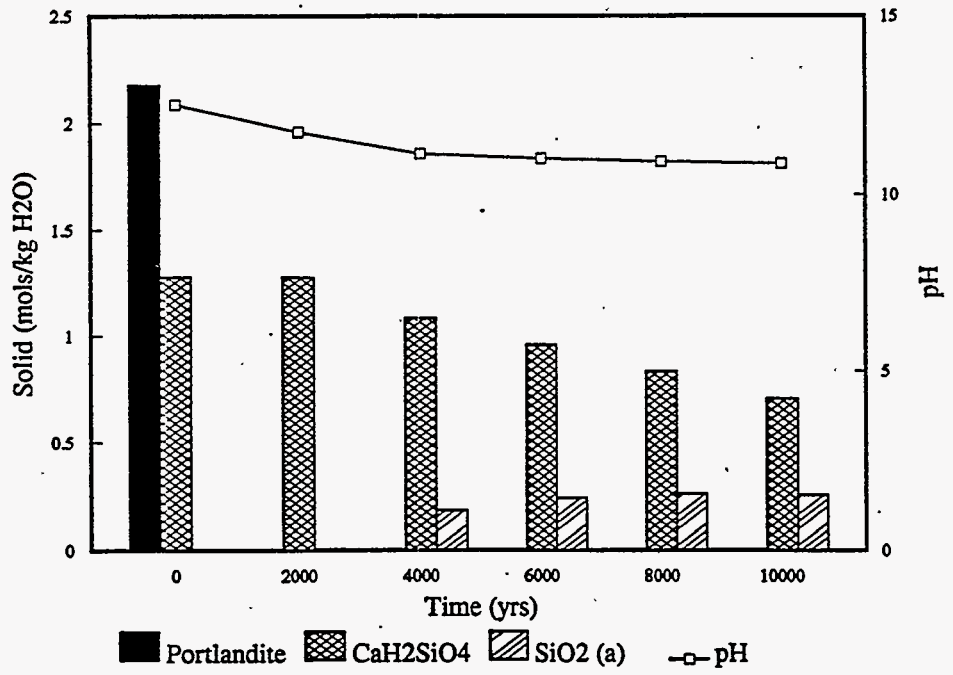

Figure 3.5b. Scenario B - Moles of Cement Present in Bin 2 (Distance) as a Function of Time

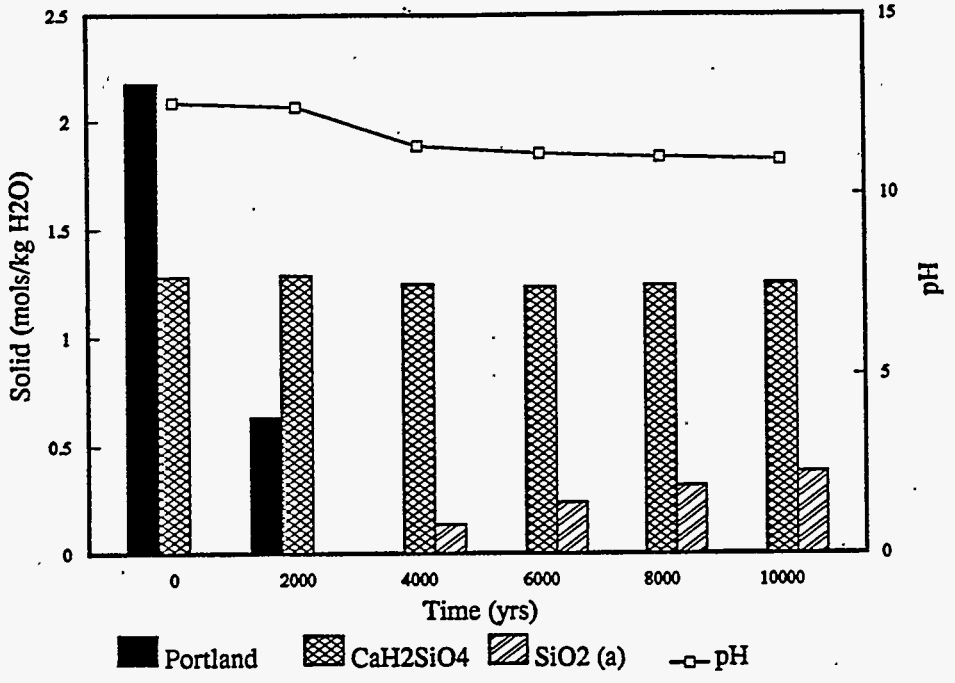

Figure 3.5c. Scenario B - Moles of Cement Present in Bin 3 (Distance) as a Function of Time

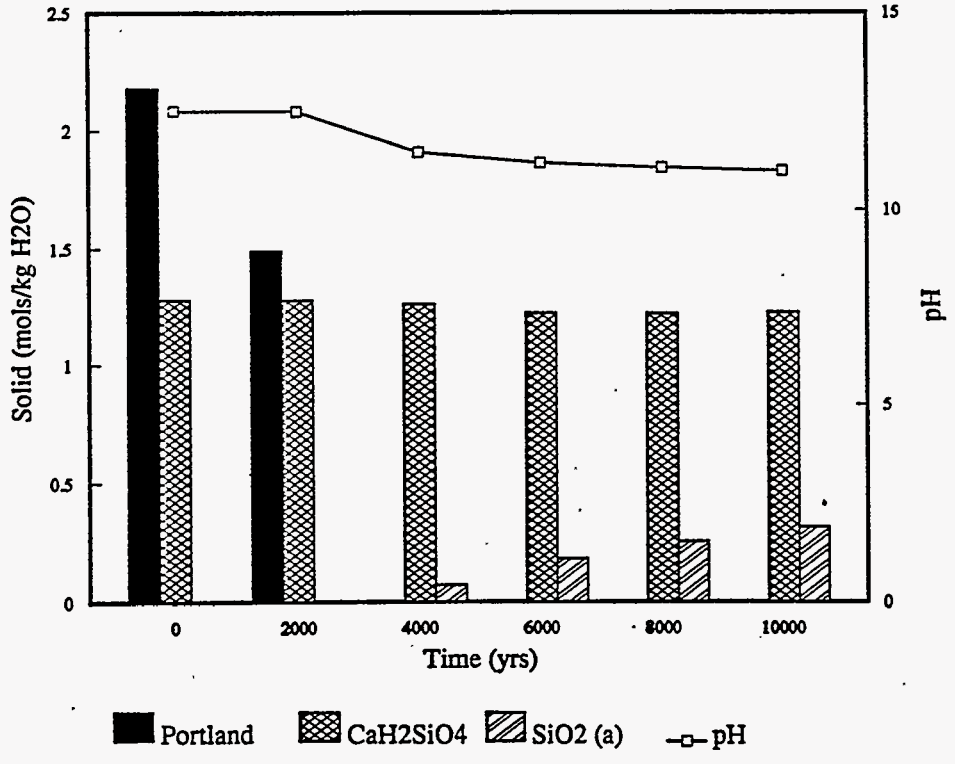

Figure 3.5d. Scenario B - Moles of Cement Present in Bin 4 (Distance) as a Function of Time

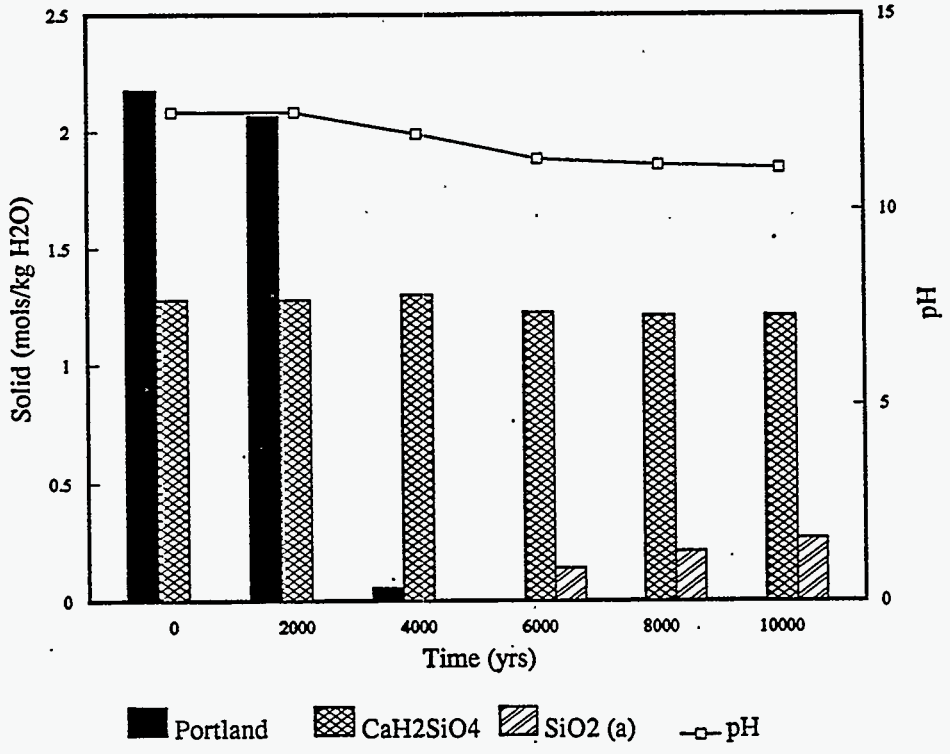

Figure 3.5e. Scenario B - Moles of Cement Present in Bin 5 (Distance) as a Function of Time

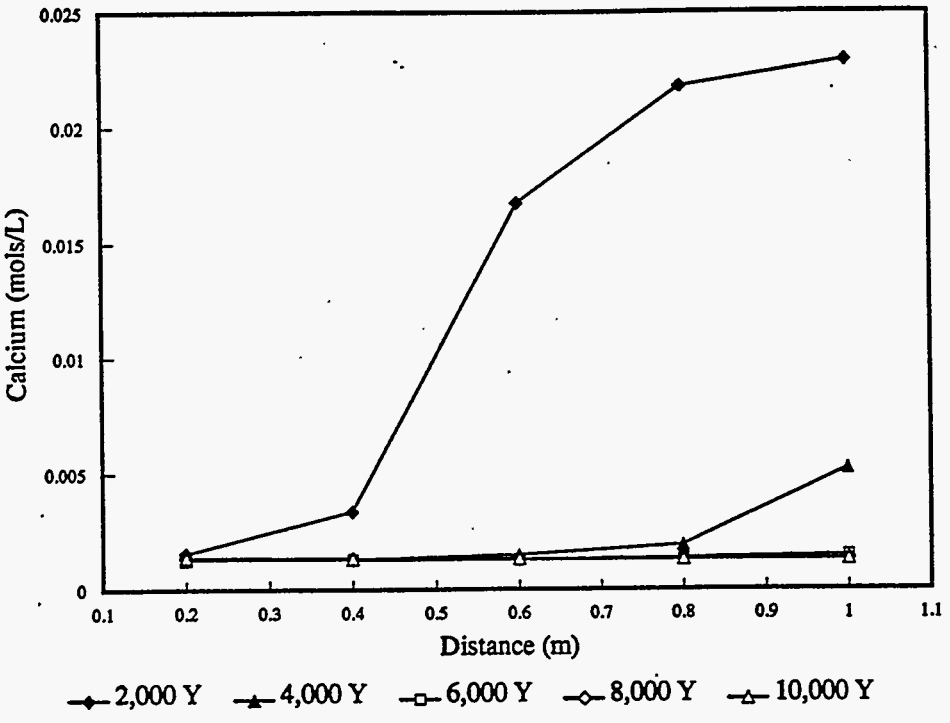

Figure 3.6a. Scenario B - Concentration of Dissolved Calcium in Porewater as a Function of Distance and Time

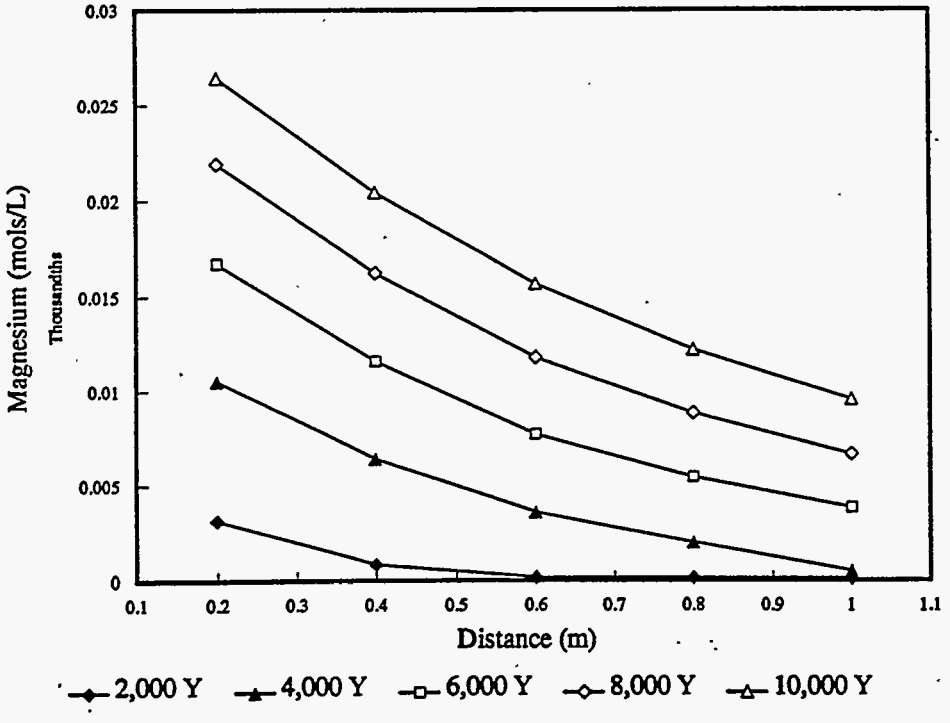

Figure 3.6b. Scenario B - Concentration of Dissolved Magnesium in Porewater as a Function of Distance and Time

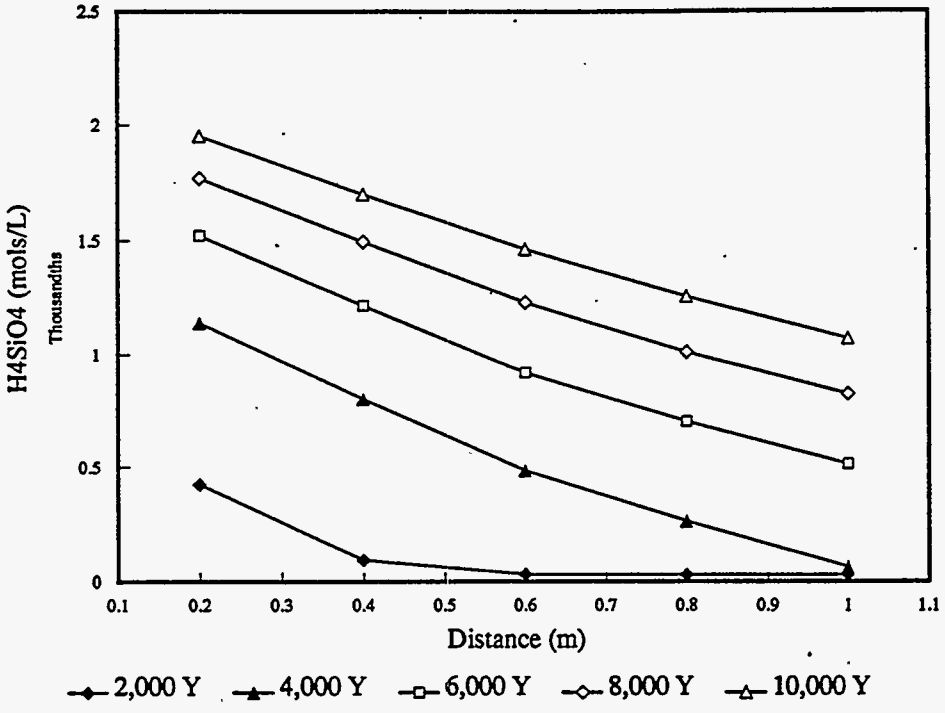

Figure 3.6c. Scenario B - Concentration of Dissolved Silica (as H_4SiO_4) in Porewater as a Function of Distance and Time

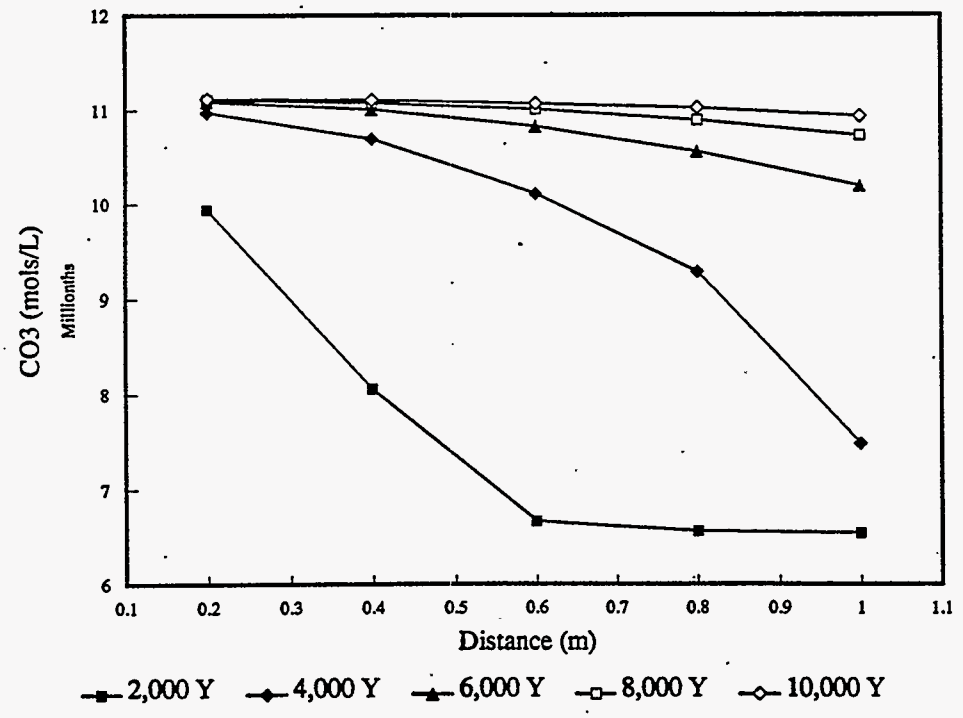

Figure 3.6d. Scenario B - Concentration of Dissolved Carbonate (CO_3) in Porewater as a Function of Distance and Time

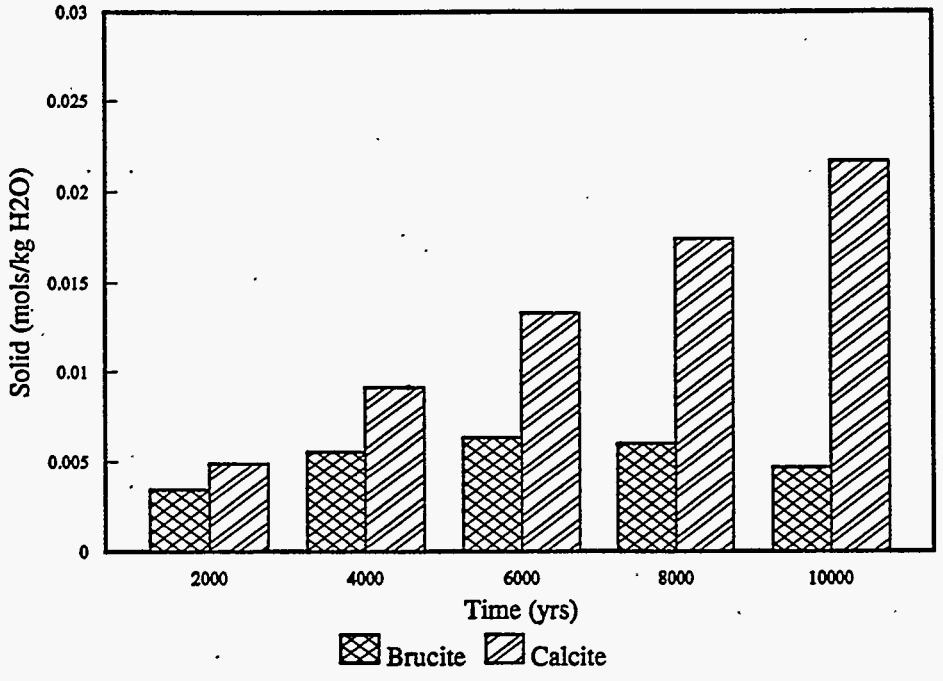

Figure 3.7a. Scenario B - Concentration of Precipitated Solids in Bin 1 as a Function of Time During Reaction Between Cement and Rainwater

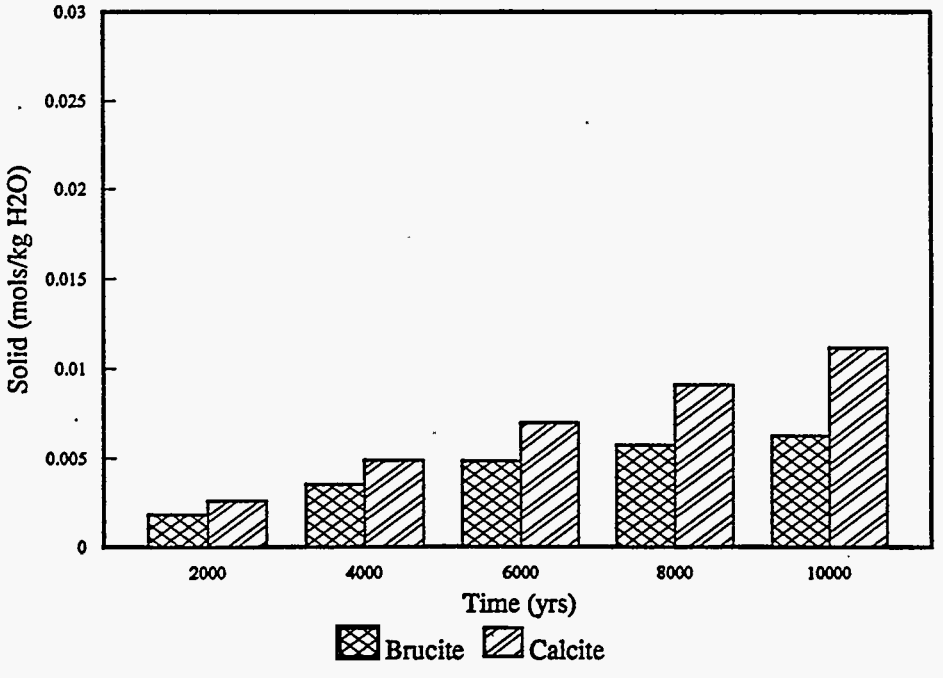

Figure 3.7b. Scenario B - Concentration of Precipitated Solids in Bin 2 as a Function of Time During Reaction Between Cement and Rainwater

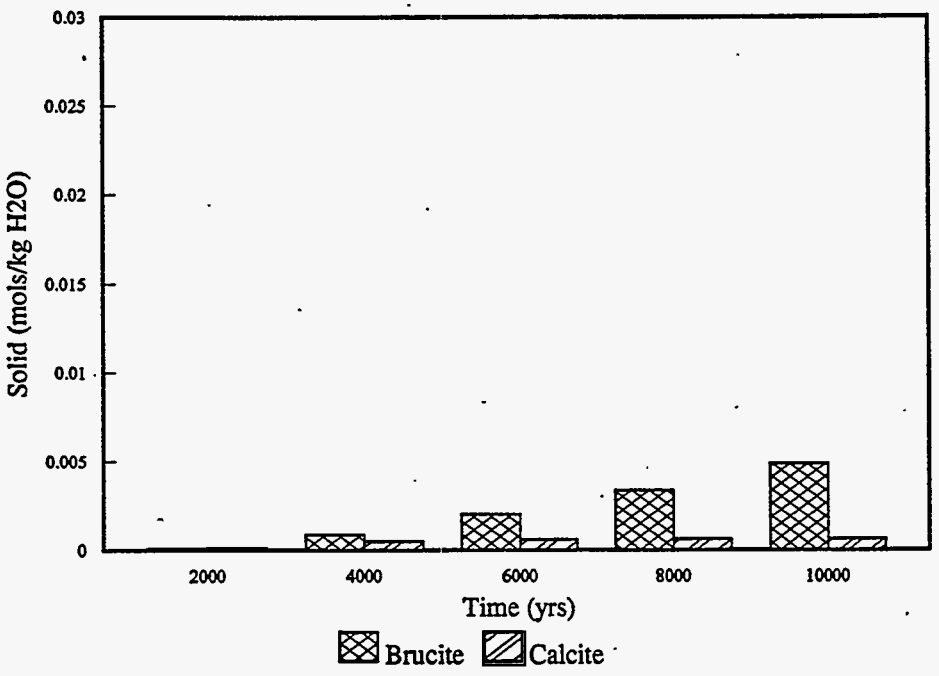

Figure 3.7c. Scenario B - Concentration of Precipitated Solids in Bin 3 as a Function of Time During Reaction Between Cement and Rainwater

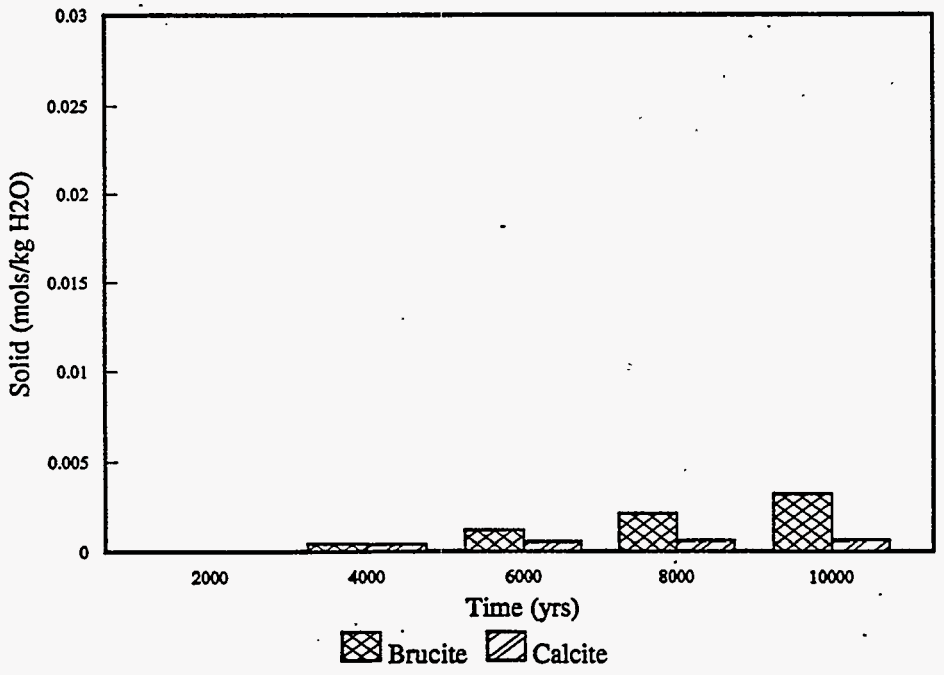

Figure 3.7d. Scenario B - Concentration of Precipitated Solids in Bin 4 as a Function of Time During Reaction Between Cement and Rainwater

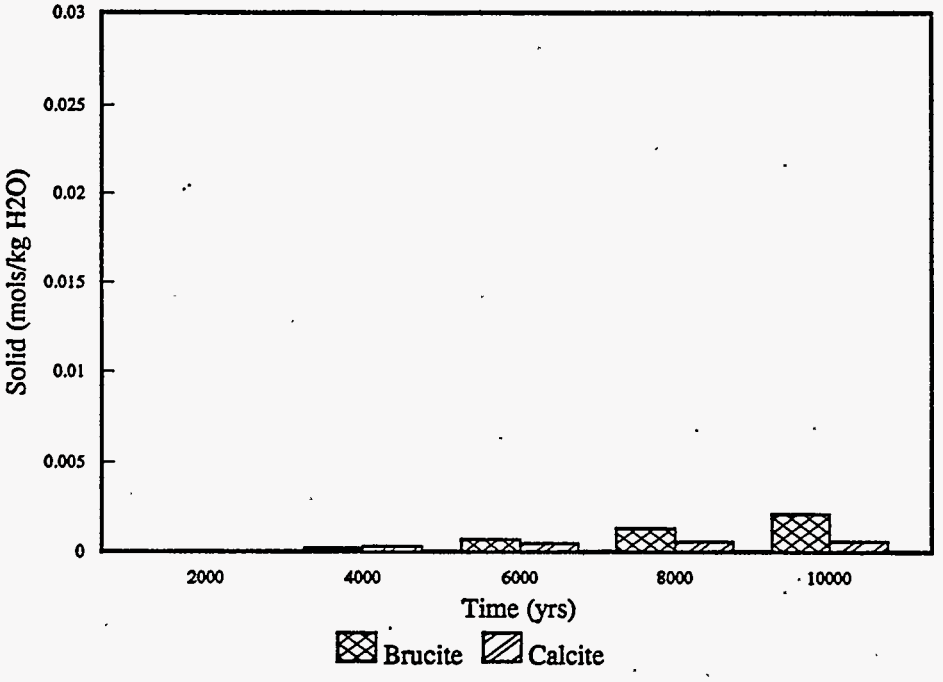

Figure 3.7e. Scenario B - Concentration of Precipitated Solids in Bin 5 as a Function of Time During Reaction Between Cement and Rainwater

3.3 Scenario D

In Scenario D, the simulated porewater from Trench 8 was used as the influent solution. Reactions between the Trench 8 porewater and cement immediately caused precipitation of brucite and calcite. Gypsum and fluorite remained undersaturated throughout the calculation. Reaction between cement and the Trench 8 porewater did not lead to cement compositions with C/S < 1; therefore the precipitation of the SiO_2 (am) end member did not occur.

In the first 0.2 m (bin 1) of the cement, the $Ca(OH)_2$ end member completely dissolved in 900 years and the pH dropped from 12.5 to 10.34. Brucite dissolved after 3,500 years and the pH was maintained at a value of 10.32 until the CaH_2SiO_4 end member completely dissolved after 8,850 years. The pH of the porewater stayed above 10 for 8,850 years, then dropped below 8 with the dissolution of CaH_2SiO_4 (Figure 3.8a). At this point, the cement [$Ca(OH)_2$ - CaH_2SiO_4] had completely dissolved and resultant porewater was identical to the initial Trench 8 porewater. The pH was controlled by calcite precipitation.

Because the Trench 8 porewater was saturated with respect to calcite and contained higher concentrations of calcium and carbonate than the rainwater, more calcite precipitated during reaction between the Trench 8 porewater and cement than upon reaction of rainwater and cement. The change of pH and concentrations of precipitated solids in bins 1 through 5 are shown in Figures 3.8a through 3.8e, respectively. In the first bin (0.2 m), in Scenario D, more than 1 mole of calcite precipitates in 10,000 years, while, in Scenario B, less than 0.025 mole of calcite precipitates during the same time period (compare Figures 3.7a and 3.8a). The precipitation of calcite from the reaction of Trench 8 porewater and cement will influence (likely reduce) the porosity of the soil/waste form in the immediate vicinity of the burial ground.

Figures 3.9a through 3.9e illustrate changes in cement porewater composition for Scenario D as a function of time and distance. The initial Ca solution concentration (Figure 3.9b) was controlled by the coexistence of the cement related solids $Ca(OH)_2$ and CaH_2SiO_4. The initial increase in moles of CaH_2SiO_4 precipitated downstream from the first bin and decrease in moles of $Ca(OH)_2$ was accompanied by an increase in Ca concentration in solution which was quickly counteracted by the precipitation of calcite which dramatically decreased the Ca solution concentration in all bins as time increased.

The CO_3 concentration (Figure 3.9c) was effectively zero in the cement porewater at the beginning of the calculation. The CO_3 concentration increased quickly to 10^{-5} mol/L and was maintained at this concentration by the coprecipitation of CaH_2SiO_4 and calcite. When the dissolution of CaH_2SiO_4 was complete, calcite became the only solubility control in the system, and both Ca and CO_3 concentrations in solution increased and were maintained at approximately 10^{-3} mol/L.

Small amounts of brucite precipitated and then redissolved through time. At 2,000 years, bins 1 and 2 contained brucite and calcite. At 4,000 years, bin 1 no longer contained brucite, and the Mg concentration in solution (Figure 3.9d) was the same as the Mg concentration present in the soil saturation extract (that is, there was no further reaction of Mg in the system).

Silicon (Si) concentrations (Figure 3.9e) are low in the cement porewater controlled by CaH_2SiO_4. When the Trench 8 porewater infiltrated the cement, the concentration of dissolved Si increased. For

8,850 years, the silica solution concentration was controlled by the presence of CaH_2SiO_4. After 8,850 years, CaH_2SiO_4 dissolved in bin 1 and the Si concentration in solution was the same as the Si concentration in the soil saturation extract.

Based on a comparison of the CTM simulations for Scenarios A and B, the rate of pH evolution appears to directly correlate with respect to the mass of cement present. Therefore, one would predict that the evolution of the porewater pH and composition for Scenario C would be the same as Scenario D. The times for the described events, however, would be approximately three times longer because Scenario C has three times as much cement as that considered in Scenario D.

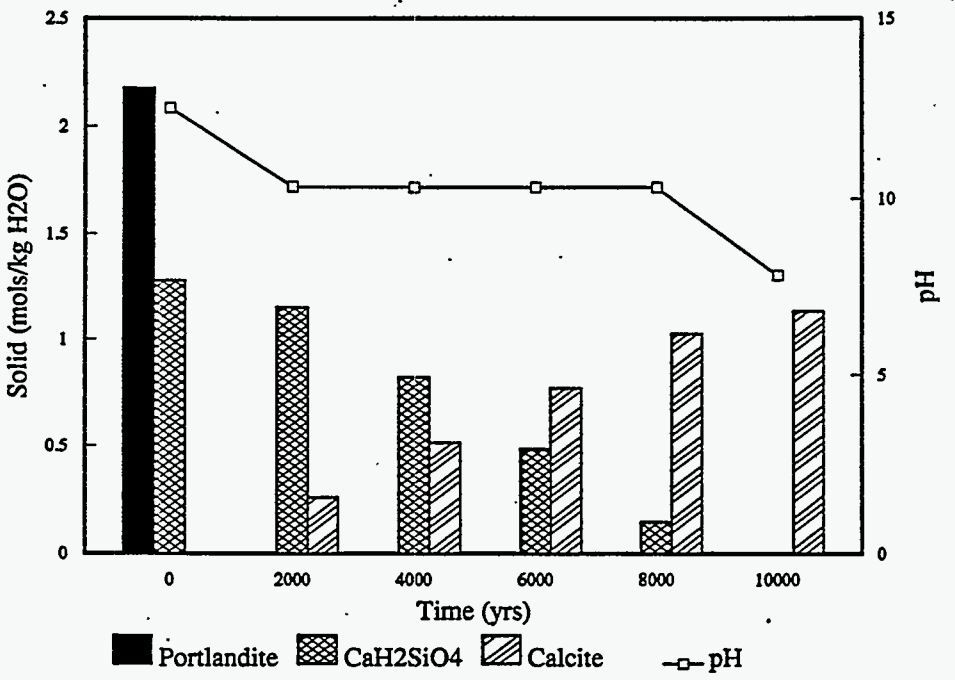

Figure 3.8a. Scenario D - pH and Concentration of Precipitated Solids in Bin 1 as a Function of Time During Reaction Between Cement and Soil Porewater

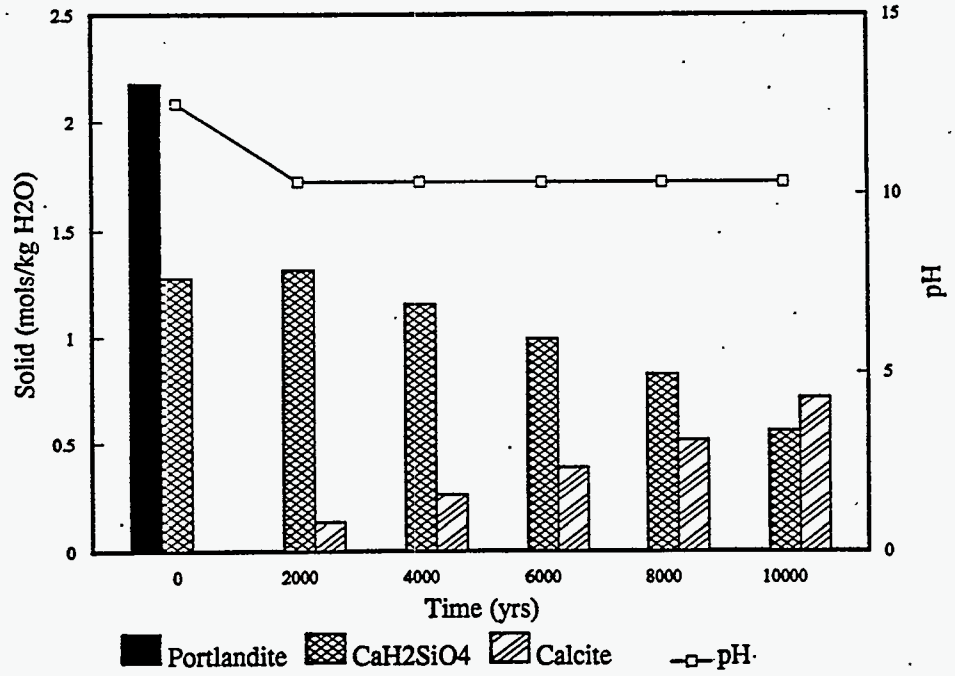

Figure 3.8b. Scenario D - pH and Concentration of Precipitated Solids in Bin 2 as a Function of Time During Reaction Between Cement and Soil Porewater

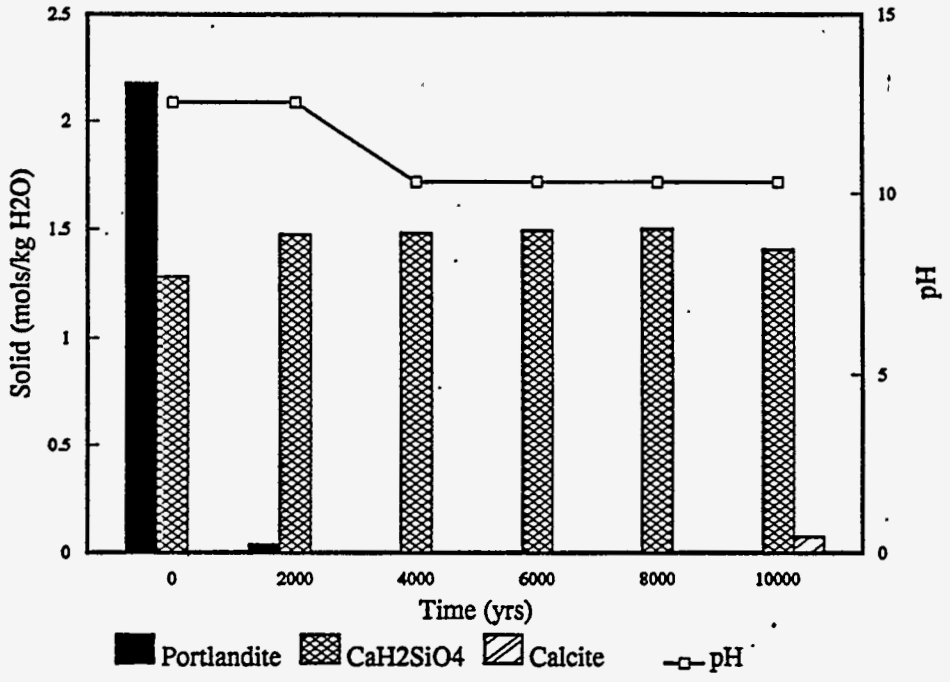

Figure 3.8c. Scenario D - pH and Concentration of Precipitated Solids in Bin 3 as a Function of Time During Reaction Between Cement and Soil Porewater

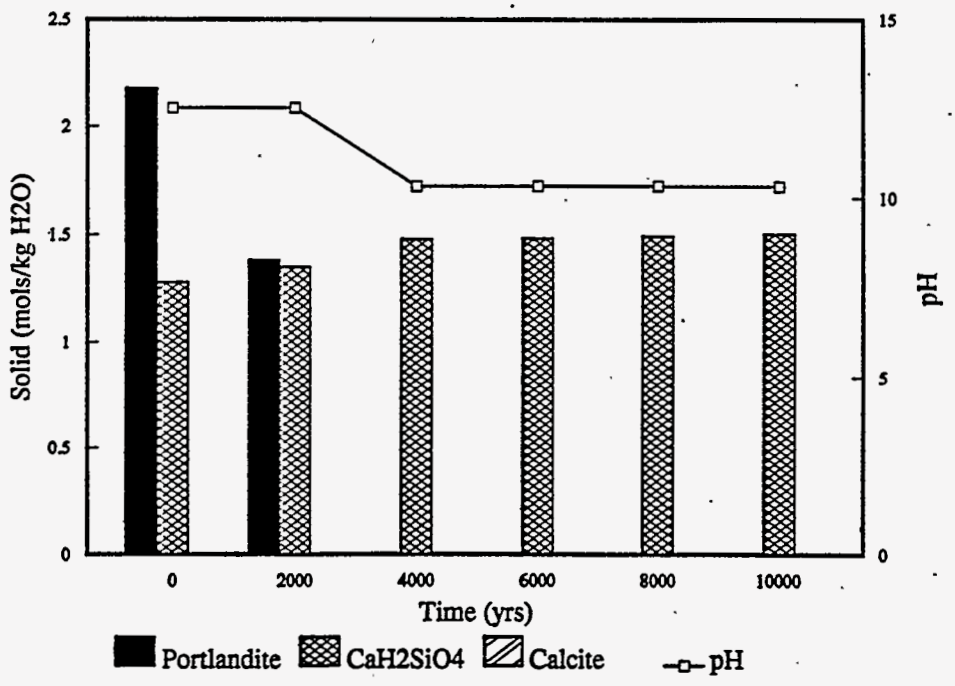

Figure 3.8d. Scenario D - pH and Concentration of Precipitated Solids in Bin 4 as a Function of Time During Reaction Between Cement and Soil Porewater

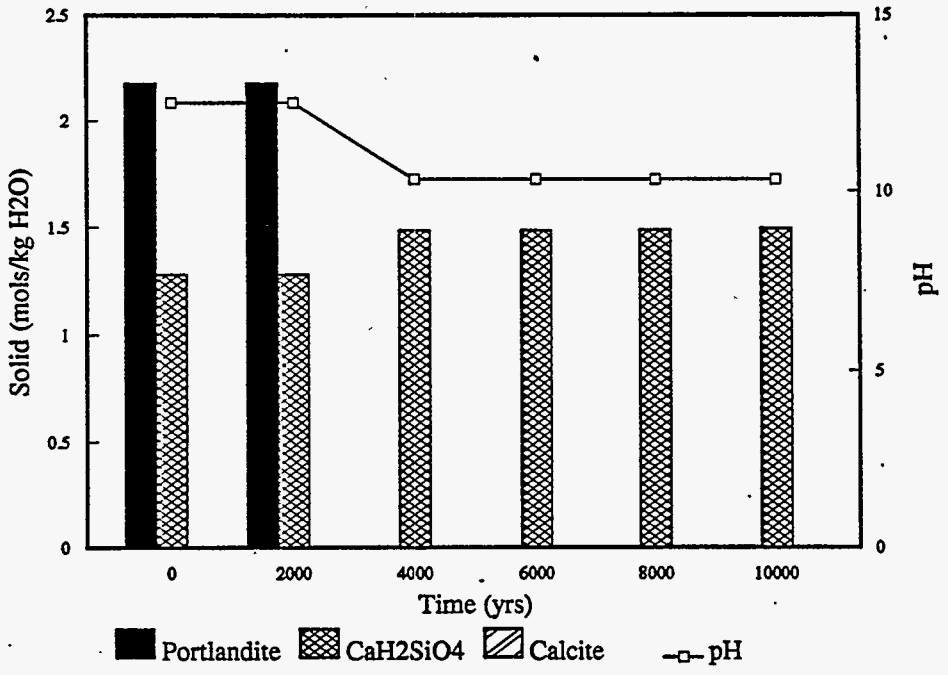

Figure 3.8e. Scenario D - pH and Concentration of Precipitated Solids in Bin 5 as a Function of Time During Reaction Between Cement and Soil Porewater

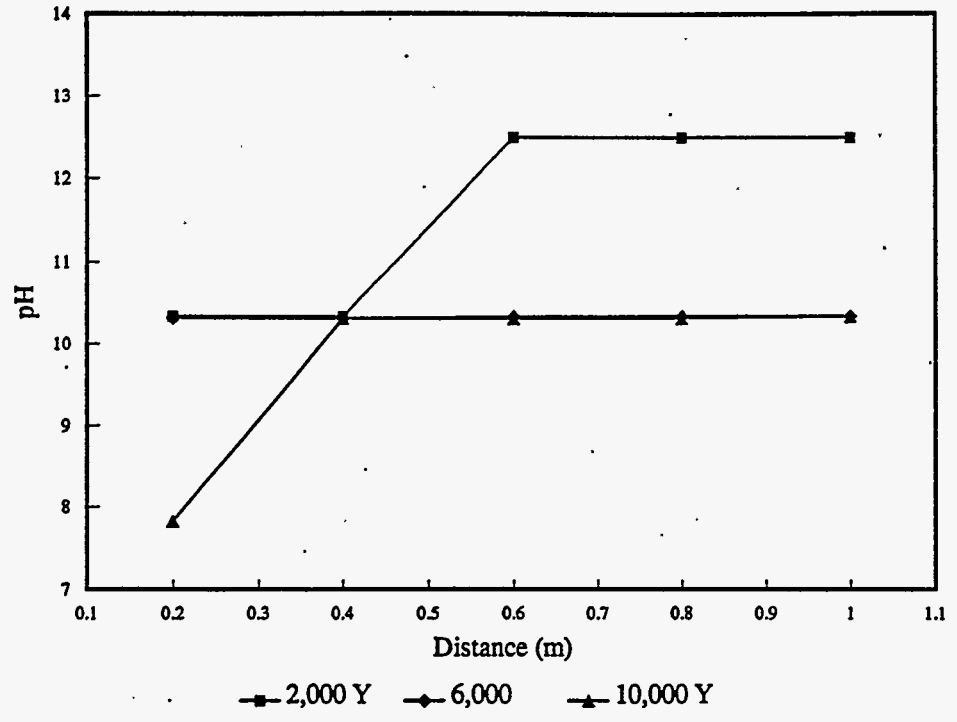

Figure 3.9a. Scenario D - pH of Porewater as a Function of Distance and Time

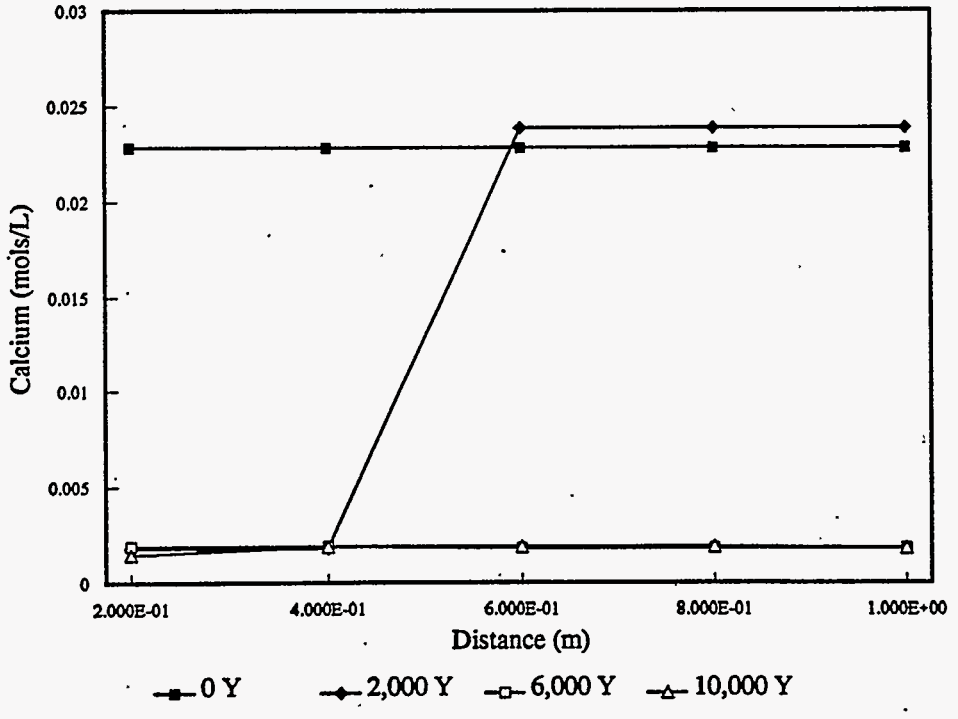

Figure 3.9b. Scenario D - Concentration of Dissolved Calcium in Porewater as a Function of Distance and Time

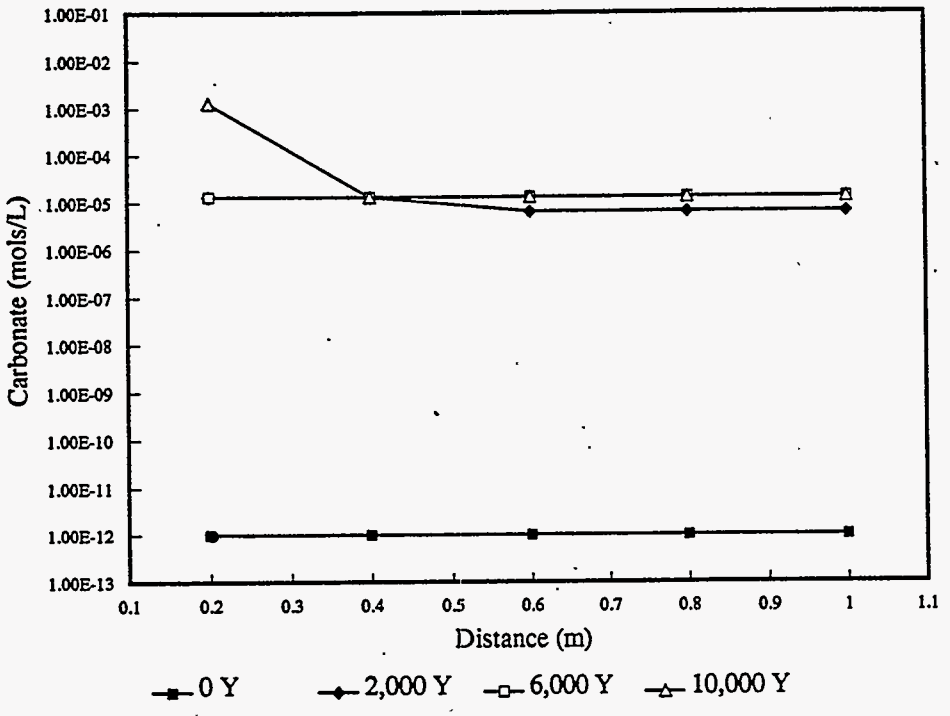

Figure 3.9c. Scenario D - Concentration of Dissolved Carbonate (CO_3) in Porewater as a Function of Distance and Time

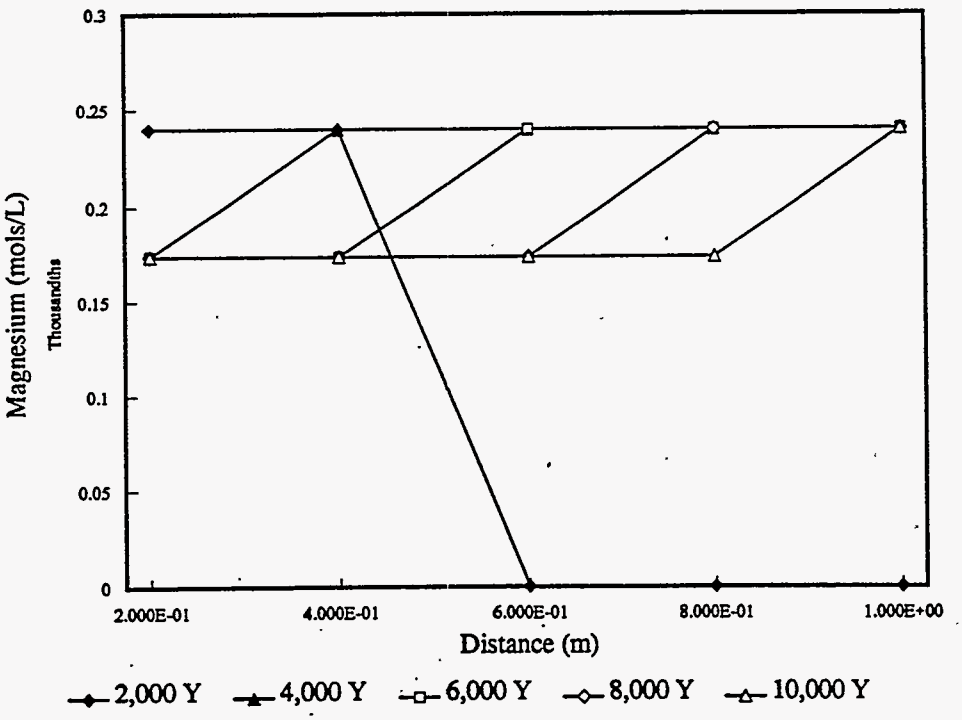

Figure 3.9d. Scenario D - Concentration of Dissolved Magnesium in Porewater as a Function of Distance and Time

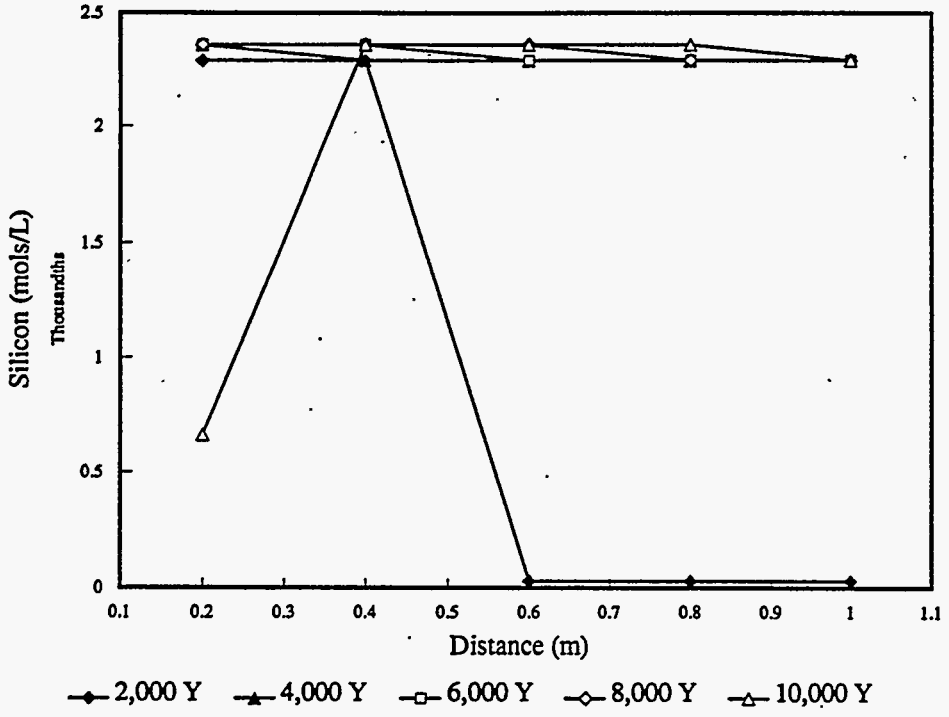

Figure 3.9e. Scenario D - Concentration of Dissolved Silicon (Si) in Porewater as a Function of Distance and Time

3.4 Summary

For the two scenarios with rainwater (coupled with barrels completely filled with cement or 1/3 filled with cement and 2/3 filled with inert waste material) and the more realistic recharge rate (0.5 cm/yr), the porewater pH in the full 1-m streamtube of cement did not decrease below a pH of 11 during 10,000 years. For the two scenarios with soil saturated extract, the porewater pH in the full 1-m streamtube did not decrease below a pH of 10 during 10,000 years. Therefore, for all four scenarios, the pH of the effluent did not decrease below a pH of 10 for the first 10,000 years. It can be extrapolated from these results that the effluent pH from a 3-m streamtube of cement (e.g., a burial ground with three barrels stacked on top of each other) will not decrease below a pH of 10 during a period of 10,000 years when the recharge rate is $\leq$0.5 cm/yr.

Because the 1-m streamtube is discretized into 5 bins, variation in the composition of the cement porewater can only be evaluated bin by bin. The change in porewater pH in the first bin or 0.2 m of cement contacted by the influent solution is provided in Table 3.1. Changes in the cement composition and porewater pH occur more slowly, when the cement reacts with rainwater than when it reacts with soil saturation extract. Within a 10,000-year period, the predicted pH in the first bin of the streamtube (0.2 m) drops below 10 for Scenario D in which the streamtube contains 1/3 cement and 2/3 inert material and the influent is soil saturation extract. For the other scenarios A-C, the calculated pH remains over 10 throughout 10,000 years. For the cases where three barrels are stacked on top of each other, one can estimate that times of events presented in Table 3.1 will increase by a factor of three.

Table 3.1. Time Predicted to Lower pH in the Outer 0.2 m of Cement Given a Recharge Rate of 0.5 cm/yr

Scenario	Influent	Barrel Contents	Time (yrs) pH > 12	Time (yrs) 10 < pH < 12
A	Rain Water	Cement	3,600	10,000
B	Rain Water	1/3 Cement 2/3 Waste	1,230	10,000
C	Soil Porewater	Cement	2,680	10,000
D	Soil Porewater	1/3 Cement 2/3 Waste	900	8,850

For a recharge rate of 5.0 cm/yr (porewater velocity of 0.25 m/yr), calculations for 3 m of cement were completed (Scenarios M through P). It is assumed that the porewater composition and solid phases present at a 1-m depth in the 3-m streamtube will be equivalent to the chemistry at the end of a 1-m streamtube. To test this hypothesis, Scenario J was modeled, and these results were compared to the results for Scenario N (see Table 3.2). The calculations for Scenarios M through P should provide information pertinent to Scenarios I through L (see Table 2.1). The results from Scenarios J and N confirm the assumption that the reaction between cement and porewater in a 1-m streamtube will parallel the reaction of cement and porewater in the first meter of a 3-m streamtube. The minor differences observed are due to different choices for bin size and time steps used for each simulation.

Table 3.2. Comparison of Scenario J and Scenario N at 1 Meter Depth in Cement

Scenario	Influent	Barrel Contents	Time (yrs) pH > 12	Time (yrs) 10 < pH < 12
J	Rain Water	1/3 Cement 2/3 Waste	440	4,110
N	Rain Water	1/3 Cement 2/3 Waste	500	4,520

For the 3-m streamtube simulations, the streamtube was divided into 15 bins, each 0.2 m in length. The results of the CTM calculations show that the porewater pH for the full 3 m of cement does not decrease below a pH of 12 in 10,000 years. Tables 3.3 and 3.4 show the results for the decrease in porewater pH at 0.2 m and 1.0 m depths into the cement. The buffering capacity of the cement is once again reduced more quickly through reaction with the soil saturation extract than through reaction with rainwater.

Table 3.3. Time Predicted to Lower pH in the Outer 0.2 m of Cement Given a Recharge Rate of 5 cm/yr

Scenario	Influent	Barrel Contents	Time (yrs) pH > 12	Time (yrs) 10 < pH < 12
M	Rain Water	Cement	720	6,560
N	Rain Water	1/3 Cement 2/3 Waste	240	2,180
O	Soil Porewater	Cement	540	5,300
P	Soil Porewater	1/3 Cement 2/3 Waste	180	1,760

Table 3.4. Time Predicted to Lower pH in the Outer 1.0 m of Cement for a Recharge Rate of 5 cm/yr

Scenario	Influent	Barrel Contents	Time (yrs) pH > 12	Time (yrs) 10 < pH < 12
M	Rain Water	Cement	1,540	10,000
N	Rain Water	1/3 Cement 2/3 Waste	500	4,520
O	Soil Porewater	Cement	1,200	10,000
P	Soil Porewater	1/3 Cement 2/3 Waste	440	3,980

4.0 Results of U(VI) Solubility Calculations

The MINTEQA2 code was used to calculate the concentrations of dissolved U(VI) for release scenarios B, D, N, and P (listed in Table 4.1) that were also modeled with CTM. These four scenarios include the two recharge rates, the two compositions of influent water, and the waste barrel content with the lower volume of cement. Additionally, three U-containing solids {schoepite ($UO_3 \cdot 2H_2O$), uranophane [$Ca(UO_2)_2(SiO_3)_2(OH)_2 \cdot 5H_2O$)], and calcium uranate ($CaUO_4$)} were included as possible solubility-controls for dissolved U(VI) for each scenario. The solution compositions predicted by CTM for bin 1 at six discrete times for each scenario were used as input for the equilibrium solubility calculations. The time steps used for the calculations were chosen where the CTM simulations indicated that pH or the mass of some cement phase changed significantly during the system evolution.

4.1 Scenario B

In Scenario B, rainwater is considered to continually percolate at a constant recharge rate of 0.5 cm/yr through a waste barrel that is 1/3 filled with cement and 2/3 filled with inert material. The pH-evolution calculations indicate that the pH of porewater in bin 1 remains at 12.5 until about 1,400 years when the $Ca(OH)_2$ component of cement is completely dissolved. At about 4,500 years, the pH is still 11 and, at the termination of the simulation (10,000 years), the pH is still elevated at 10.81.

The predicted concentrations of dissolved U(VI) varies significantly with pH and the choice of solubility-controlling solid. A summary of the MINTEQA2 calculations for Scenario B is listed in Table 4.1. When schoepite is assumed to be the solubility-controlling solid, the concentration of dissolved U(VI) in the effluent is initially high and then decreases as pH of the porewater decreases with time. During the initial stages of cement dissolution in Scenario B when the pH is 12.5, the solution concentration of U(VI) is predicted to be 1.8×10^{-2} M (~4,300 ppm). After 10,000 years, when the pH has decreased to 10.81, the U concentration is predicted to be 2.9×10^{-4} M (~70 ppm).

If uranophane is assumed to be the solubility-controlling solid, the trend is similar in that the solution concentration of U(VI) is higher during early stages of cement dissolution when the pH is highest, and lower at the end of the 10,000 years when pH has decreased somewhat. Although the trend is similar, the concentration of dissolved U(VI) predicted using the solubility of uranophane is significantly lower than that based on the solubility of schoepite. Assuming equilibrium between the CTM-predicted composition of the porewater in bin 1 and uranophane, the total U(VI) solution concentration is predicted to be 4.3×10^{-6} M (~1 ppm) at pH 12.5 and 3.5×10^{-10} M (~0.06 ppb) at the end of 10,000 years at pH 10.81. This major decrease in the concentration of dissolved U(VI) is mostly due to the dramatic increases in the concentration of dissolved silica as the C-S-H cement gel dissolves, which, in turn, lowers the mass of U(VI) that can be in solution in equilibrium with the silica-bearing uranophane.

The lowest concentrations of dissolved U(VI) at each time step are predicted when calcium uranate is assumed to be the solubility-controlling solid for dissolved U(VI). Initially, when the porewater has the highest pH, calcium uranate is least soluble because the concentrations of dissolved Ca are the highest. At the end of the CTM simulations when solution concentrations of Ca are lower,

calcium uranate is more soluble but would still control the U(VI) concentrations in solution at a very low values of 1.1×10^{-11} M (~0.003 ppb).

For all the MINTEQA2 calculations involving Scenario B, 91-99% of the dissolved U(VI) at these high pH values is predicted to be present as the aqueous species $UO_2(OH)_3^-$. Most of the remaining dissolved U(VI) will exist as the species $UO_2(OH)_2^0$ (aq) and $(UO_2)_3(OH)_7^-$. The exact percentages of each species depends on the pH of the porewater.

Table 4.1. Concentrations of Dissolved U(VI) Versus pH/Time for Selected Solubility-Controlling Solids for Scenarios B and D Based on 1/3 Barrel of Cement and Two Types of Influent Solutions

Solubility-Controlling Solid	Concentration of Dissolved U(VI) in Effluent mol/L and (*ppm*)			
Scenario B (Porewater Velocity: 0.5 cm/yr, Influent: Rain)				
	pH 12.5 at 0 - 1,400 yrs	pH 11.75 at 1,410 yrs	pH 10.99 at 4,480 yrs	pH 10.81 at 10,000 yrs
Schoepite	1.8×10^{-2} ($4.3 \times 10^{+3}$)	2.6×10^{-3} ($6.3 \times 10^{+2}$)	4.4×10^{-4} ($1.0 \times 10^{+2}$)	2.9×10^{-4} ($7.0 \times 10^{+1}$)
Uranophane	4.3×10^{-6} (*1.0*)	6.9×10^{-8} (1.6×10^{-2})	6.3×10^{-10} (1.5×10^{-4})	2.5×10^{-10} (6.0×10^{-5})
Ca Uranate	4.1×10^{-14} (9.7×10^{-9})	6.6×10^{-13} (1.6×10^{-7})	7.8×10^{-12} (1.9×10^{-6})	1.1×10^{-11} (2.6×10^{-6})
Scenario D (Porewater Velocity: 0.5 cm/yr, Influent: Soil Porewater)				
	pH 12.5 at 0 - 850 yrs	pH 12.13 at 890 yrs	pH 10.32 at 3,360 yrs	pH 7.83 at 9,460 yrs
Schoepite	1.8×10^{-2} ($4.3 \times 10^{+3}$)	6.9×10^{-3} ($1.6 \times 10^{+3}$)	9.9×10^{-5} ($2.4 \times 10^{+1}$)	9.8×10^{-5} ($2.3 \times 10^{+1}$)
Uranophane	4.4×10^{-6} (*1.0*)	6.2×10^{-7} (1.5×10^{-1})	7.3×10^{-11} (1.7×10^{-5})	1.0×10^{-8} (2.5×10^{-3})
Ca Uranate	4.0×10^{-14} (9.6×10^{-9})	1.5×10^{-13} (3.5×10^{-8})	3.1×10^{-11} (7.3×10^{-6})	1.7×10^{-6} (4.1×10^{-1})

4.2 Scenario D

The MINTEQA2 solubility calculations for Scenario D includes the soil porewater extract for the Hanford vadose zone sediment as the composition of the initial influent, the recharge rate of 0.5 cm/yr, and a waste barrel with a 1/3 cement content. The modeling results for the early time periods are very similar to the results for Scenario B. The interaction of the soil porewater with the cement causes the pH to decrease (decreasing from a value of 12.5 as the $Ca(OH)_2$ component is removed) more rapidly than when rainwater is the reacting influent. The pH of the porewater in bin 1 has decreased to 10.3 after approximately 3,500 years and 7.8 after approximately 9,500 years. At 9,500 years, the system is essentially devoid of cement solids and the composition of the porewater is identical to the soil saturation extract. No further reactions are then expected. This final pH of 7.8 is significantly different when compared to the CTM results for rainwater as the influent (Scenario B) where the pH of the porewater in bin 1 does not decrease below 10.8 even after 10,000 years.

The solubility predictions of dissolved U(VI) for Scenario D are summarized in Table 4.1. The larger change in porewater pH in Scenario D causes a larger difference in the predicted concentrations of dissolved U(VI). The general trend in U(VI) solubility predicted for Scenario B is also observed for the modeling results for Scenario D where the calculated concentrations of dissolved U(VI) based on the solubilities of schoepite and uranophane decrease as time progresses and the porewater pH decreases, whereas those based on the solubility of calcium uranate increase with time and decreasing pH. At a pH value of 12.5, schoepite is rather soluble [4,300 ppm total dissolved U(VI)], uranophane is moderately soluble [~1 ppm total dissolved U(VI)], and calcium uranate is very insoluble [$\sim 1 \times 10^{-8}$ ppm total dissolved U(VI)].

After approximately 9,500 years, when all of the CSH-gel have been leached, the predicted concentrations of dissolved U(VI) for a porewater pH of 7.8 are 9.8×10^{-5} M (23 ppm), 1.0×10^{-8} M (0.002 ppm), and 1.7×10^{-6} M (0.4 ppm), respectively, for the solubilities of schoepite, uranophane and calcium uranate. For this cement-water system (Scenario D) at the pH of 7.8, uranophane is the least soluble solid as compared to Scenario B in which calcium uranate was the least soluble solid.

For Scenario D, the dissolved U(VI) is also present predominately as the aqueous species $UO_2(OH)_3^-$ until the pH decreases to 7.8. At this low pH, uranyl carbonate and mixed hydroxy-carbonate complexes [$(UO_2(CO_3)_2^{2-}$, $UO_2(CO_3)_3^{4-}$, and $(UO_2)_2CO_3(OH)_3^-$] are the predominant aqueous forms of dissolved U(VI).

4.3 Scenario N

The concentrations of dissolved U(VI) predicted with MINTEQA2 for Scenario N can be compared to those for Scenario B, because the two scenarios differ only in the assumed recharge rate with the flow rate of infiltrating rainwater for Scenario N being ten times greater. The $Ca(OH)_2$ component of the CSH-gel disappears from the waste form in Scenario N approximately five times faster than in the Scenario B calculations. The porewater pH remains at 12.5 until $Ca(OH)_2$ has completely dissolved. The pH then starts to decrease more quickly in Scenario N, and all traces of cement and its reaction products have totally leached from the system after about 2,200 years. At this point, calcite is the only phase that remains to buffer the pH, and, by 2,500 years, the system has reached the pH (5.9) of the rainwater influent.

Until about 2,000 years, the MINTEQA2 predictions for Scenario N of the solubility of dissolved U(VI) are very similar to those for Scenario B, except for the time for corresponding chemical changes in Scenario N being approximately five times shorter. After 2,000 years, the pH of the porewater for Scenario N has decreased below any value predicted in Scenario B. At about 2,200 years, when the porewater pH is ~9.7, the predicted concentration of dissolved U(VI) is 7.8, 0.012, or 0.0003 ppm, respectively, depending upon if schoepite, uranophane, or calcium uranate is assumed to be the solubility-controlling solid. At 2,520 years, when the system is completely leached of cement and the pH is 5.9, the predicted concentrations of dissolved U(VI) are 1.2, 5.5, or 4,500 ppm, respectively, depending of the same sequence of solubility-controlling solids. These results are summarized in Table 4.2.

Table 4.2. Solution Concentrations of U(VI) Versus pH/Time for Selected Solubility-Controlling Solids for Scenarios N and P Based on 1/3 Barrel of Cement and Two Types of Influent Solutions

Solubility-Controlling Solid	Concentration of Dissolved U(VI) in Effluent mol/L and (*ppm*)			
Scenario N (Porewater Velocity: 5 cm/yr, Influent: Rain)				
	pH 12.5 at 0 - 250 yrs	pH 11.63 at 280 yrs	pH 9.73 at 2,180 yrs	pH 5.90 at 2,520 yrs
Schoepite	1.8×10^{-2} ($4.2 \times 10^{+3}$)	2.0×10^{-3} ($4.7 \times 10^{+2}$)	3.3×10^{-5} (7.8)	5.1×10^{-6} (1.2)
Uranophane	4.3×10^{-6} (1.0)	3.0×10^{-8} (7.2×10^{-3})	5.1×10^{-8} (1.2×10^{-2})	2.3×10^{-5} (5.5)
Ca Uranate	4.1×10^{-14} (9.8×10^{-9})	1.1×10^{-12} (2.5×10^{-7})	1.2×10^{-9} (3.0×10^{-4})	1.9×10^{-2} ($4.5 \times 10^{+3}$)
Scenario P (Porewater Velocity: 5 cm/yr, Influent: Soil Porewater)				
	pH 12.5 at 0 - 50 yrs	pH 12.13 at 160 yrs	pH 10.32 at 640 yrs	pH 7.83 at 1,760 yrs
Schoepite	1.8×10^{-2} ($4.3 \times 10^{+3}$)	6.9×10^{-3} ($1.6 \times 10^{+3}$)	9.9×10^{-5} ($2.4 \times 10^{+1}$)	9.8×10^{-5} ($2.3 \times 10^{+1}$)
Uranophane	4.4×10^{-6} (1.1)	6.2×10^{-7} (1.5×10^{-1})	7.3×10^{-11} (1.7×10^{-5})	1.0×10^{-8} (2.5×10^{-3})
Ca Uranate	4.0×10^{-14} (9.7×10^{-9})	1.5×10^{-13} (3.5×10^{-8})	3.1×10^{-11} (7.3×10^{-6})	1.7×10^{-6} (4.1×10^{-1})

4.4 Scenario P

The final suite of MINTEQA2 calculations were completed using porewater compositions for Scenario P predicted with the CTM code. The conditions for this scenario differ from those for Scenario D only in assumed recharge rate, and from those for Scenario N in the composition of the influent reacting with the cementitious, U-bearing waste. The total concentrations of dissolved U(VI) and distribution of U(VI) aqueous species calculated for Scenario P are the same as those described above for Scenario D. Although the chemical systems used to simulate Scenarios D and P are the same, the factor of ten increase in recharge rate used for Scenario P results in a factor of five decrease in the times calculated for major changes in the chemistry of the cement/porewater system. At each corresponding major change in the evolution of the porewater pH out to the time when all cement components have dissolved, the predicted concentrations of dissolved U(VI) for Scenario P from 0 to 1,760 years (Table 4.1) are approximately the same as those for Scenario D from 0 to 9,460 years, including the types of solubility-controlling solids.

4.5 Summary

At the early period of cement/porewater reaction, the $Ca(OH)_2$ component of the CSH-gel controls the porewater composition and pH at 12.5. Under these conditions, the concentrations of dissolved U(VI) should be less than 1 ppm if controlled by calcium-bearing uranyl silicates or in the low ppb range if controlled by calcium uranate-like solids. At intermediate times, when porewater pH is controlled in the range of 10.9 to 12.5 by the cement CSH-gel, the solution concentrations of U(VI) should be in the low ppb to 100's of ppb range. After the cement components have all dissolved and the porewater pH is controlled at values near 7.8-8.5 by calcite or reactions with other major secondary minerals, the MINTEQA2 calculations indicate that schoepite would limit the concentrations of dissolved U(VI) in the range of 1 to 25 ppm. On the other hand, if calcium uranate or uranophane is the solubility control at these near-neutral or slightly acidic pH values, the solution concentration of U(VI) would be approximately 1 ppm or in the low ppb range, respectively.

5.0 Conclusions

5.1 Evolution of Porewater pH and Cement Degradation

The coupled/reactive transport calculations using the CTM model demonstrate that, over time, the portlandite [$Ca(OH)_2$] component of the CSH-gel dissolves completely by reaction with the influent solution. Depending on the influent composition, the SiO_2 (am) component may be introduced. The cement degrades more quickly when it reacts with the soil porewater (characteristic of Trench 8 porewater) than when it reacts with rainwater. Calcite ($CaCO_3$) and brucite [$Mg(OH)_2$] precipitate during a 10,000-year period. The pH of the porewater decreases below 10 when the CaH_2SiO_4 component of CSH-gel completely dissolves.

The CTM calculations also predict that, regardless of which recharge rate and influent are considered, the CaH_2SiO_4 component will not completely dissolve within 10,000 years from Fe barrels that are filled entirely with Portland Type I cement. For a 1-m high Fe barrel that is only 1/3-filled with cement, the results predict that, given a 0.5 cm/yr recharge rate, the CSH-gel will not completely dissolve in 10,000 years. Therefore, the porewater pH will remain above 10 for at least 10,000 years.

On the other hand, at a faster recharge rate of 5 cm/yr for either influent solution, the components of the CSH-gel are predicted to completely dissolve after 4,000 years in the 1-m high Fe-barrel that is only 1/3-filled with Portland Type I cement. The porewater pH decreases below 10 after 4,520 and 3,980 years for rainwater influent and soil saturation extract, respectively, reacting with the cement waste form. As the cement reacts with the soil porewater, the following major solid phase assemblages form in sequence: 1) CaH_2SiO_4, brucite and calcite; 2) CaH_2SiO_4 and calcite; and 3) calcite. The sequence of solid phase assemblages that occur from reaction between cement and rainwater is: 1) CaH_2SiO_4-SiO_2 (am), calcite, and brucite; 2) calcite and brucite; 3) calcite; and 4) no solids present. In either case, at the 5 cm/yr recharge rate, after 4,000 to 4,500 years, the pH of porewater inside the 1-m thick weathered waste form will be the same as that of the influent solution. If three drums were stacked on top of each other, the cement would not all dissolve and the porewater pH value would not decrease below 10 for the entire 10,000 year period modeled. However, the upper two barrels should be completely devoid of cementitious solids by the end of 10,000 years for the upper bound recharge rate of 5 cm/yr.

5.2 Solubility Limits for Dissolved U(VI)

As long as the hydration components of the CSH-gel are present in the cement, the pH of the surrounding porewater will remain greater than 10. Based on equilibrium thermodynamic considerations, the most likely U-bearing solids that should be present as solubility controls for dissolved U(VI) present are quite insoluble at pH values above 10. Total concentrations of dissolved U(VI) should be in the sub-ppb (parts per trillion) to at most 1 ppm under these CSH-gel dominated conditions. After the components of the CSH-gel have all been dissolved by the porewater, the total U(VI) solution concentrations would be controlled at the ambient porewater pH by U-bearing solids such as schoepite, uranyl silicates, or perhaps alkaline-earth uranates. The uranyl silicates are less soluble than the alkaline earth uranates and schoepite at slightly alkaline to neutral pH values as expected for the Hanford scenarios modeled in this study. Uranyl silicates would limit the concentrations of dissolved U(VI) to the low ppb range. Calcium uranate would control solution

concentrations of U(VI) to the range from 100s of ppb to low ppm, while schoepite would limit U(VI) solution concentrations to the range several ppms to several tens of ppm.

The concentration limits predicted for dissolved U(VI) using the MINTEQA2 code were based on assuming one of three U-bearing solids is the solubility control. The thermodynamic databases of MINTEQA2 and other geochemical reaction codes include a large suite of U(VI)-bearing solids (for example, see U-containing solids listed in the appendix). An examination of all the possible solids that could control the concentrations of dissolved U(VI) indicates that another uranyl silicate mineral, such as soddyite [$(UO_2)_5(SiO_4)_2(OH)_2 \cdot 5H_2O$], could be a candidate solubility-controlling solid for dissolved U(VI). Soddyite is slightly less soluble than schoepite ($UO_3 \cdot 2H_2O$) at high pH values, and much more insoluble at neutral pH conditions. Our modeling calculations indicate that soddyite is however more soluble than uranophane [$Ca(UO_2)_2(SiO_3)_2(OH)_2 \cdot 5H_2O$)] under all conditions. Therefore, at the pH conditions predicted in this study, the solubility of soddyite is intermediate relative to those of schoepite and uranophane. For a pH greater than 8, soddyite is always much more soluble than calcium uranate ($CaUO_4$). However, for porewater pH values less than approximately 8, all the U(VI)-bearing minerals considered in these MINTEQA2 calculations, including soddyite, are less soluble than calcium uranate. Another way of stating this relationship is that calcium uranate can only be the most stable solid at pH values greater than 8. If we had completed more modeling simulations in the pH region from 7.8 to 9.7, the minimum pH for the stability limit of calcium uranate might even be further restricted to a pH value above 9. The MINTEQA2 calculations also indicate that another uranyl silicate, haiweeite [$Ca(UO_2)_2Si_6O_{15} \cdot 5H_2O$], is more stable than uranophane and soddyite in the mid pH range from approximately 10.4 to neutral pH values, but very soluble above pH 10.5.

Based on empirical observations from laboratory leach experiments with cementitious materials present (for example, see Atkins and Glasser 1992; Atkins et al. 1990 1991; Brownsword et al. 1990; and Serne et al. 1989) and solubility tests of U(VI)-bearing solids at alkaline to neutral pH conditions (for example see Brush 1980 and Krupka et al. 1985), it seems likely that a transition/transformation of U(VI)-solubility controlling solids may occur as the cement chemistry and pH evolve in environments analogous to the hypothetical Hanford solid waste scenarios considered in this study. That is, it is very likely that different U solids will control the concentration of dissolved U(VI) during the different stages of the evolution of the porewater pH and composition. We speculate that solids similar to calcium uranate control the concentrations of dissolved U(VI) in porewater at the very high pH values associated with fresh cement and excess $Ca(OH)_2$ (pH = 12.5). Calcium uranate or uranyl silicates, such as uranophane, will control the concentration of dissolved U(VI) at intermediate alkaline conditions (pH's ~11 down to 8 or 9), and then perhaps schoepite becomes the solubility-controlling solid at pH values below 8 or 9.

These possibilities lead to the following predictions. At early times, when $Ca(OH)_2$ controls the cement chemistry and pH (12.5), the concentrations of dissolved U(VI), if controlled by calcium uranate-like solids, should be in the low ppb range or, at most, less than 1 ppm if controlled by calcium bearing uranyl silicates. At intermediate times, where pH is controlled by the components of the cement CSH-gel, U(VI) solution concentrations should be in the low ppb to 100s of ppb range. After all of the CSH-gel components have dissolved and the composition of the porewater is controlled by calcite or reactions with other major secondary minerals, schoepite would limit concentrations of dissolved U(VI) to the range of 1 to 25 ppm. If calcium uranate or uranophane was still the U(VI)-controlling solid at ambient pH conditions, the concentrations of dissolved U(VI) would be near 1 ppm or in the low ppb range, respectively.

5.3 Recommended Future Studies

The following future studies are recommended:

- Coupled reaction/transport modeling calculations to examine changes in porosity due to cement dissolution
- Sensitivity analysis of hydrodynamic dispersion to study its affect on the concentrations of dissolved constituents in the porewater
- Detailed laboratory studies of the solubility of well characterized U(VI) solids in environmentally relevant waters across the pH range from 7 to 12.5 to help validate the geochemical modeling calculations.

It is evident from results presented in Figures 3.5 and 3.8 that the mass of the CSH-gel components present in the streamtube (simulating the hydration and weathering of a radioactive waste form within a shallow land burial ground) changes substantially with time. Calculations to examine changes in porosity due to cement dissolution may be important to this study, because an increase in porosity will lead to a lower solid/water ratio and potentially to a faster rate of cement dissolution. Future work should also include a sensitivity analysis of hydrodynamic dispersion on the concentrations of dissolved constituents in the porewater.

Experimental studies where specific uranium (VI) solids have been used or identified in shallow land burial grounds or cement waste forms are quite limited. There is only empirical data available for concentrations of dissolved U(VI) in the presence of cement leachates. In general, the U(VI) solution concentrations are found to be less than tens of ppb to less than one ppm which are in good agreement with our modeling predictions. Other studies of the solubility of schoepite in simple solutions that do not include dissolved silica or carbonate are available that confirm the adequacy of thermodynamic data in the MINTEQA2 database for schoepite. However, more detailed laboratory studies using well characterized U(VI) solids and environmentally relevant waters across the pH range from 7 to 12.5 are recommended to evaluate the veracity of these MINTEQA2 predictions. Extra attention should be placed on monitoring possible transformations of U(VI) solid and the equilibrium pH and solution concentrations of Ca, Si and other alkaline earth and alkali metal elements. Empirical solubility data for uranyl silicates and uranyl alkaline-earth and alkali metals, such as Ca, Mg, Na and K, are not available. These four cations in addition to silica are naturally present in soil porewaters. Laboratory-scale solubility experiments where the presence of these constituents may form U(VI)-bearing solids need to be performed to fully verify calculations such as those presented in this report. The dissolution of cement hydration products especially result in significant quantities of dissolved Ca, Na, K and Si being added to the porewaters. Under these conditions, the formation of less soluble uranyl silicates, calcium uranyl silicates, and/or alkaline earth uranates are very plausible. For conservative bounding calculations at near-neutral pH conditions, concentrations of dissolved U(VI) controlled by the solubility of the oxide schoepite remains a technically defensible approach. Only, if more realistic solubility calculations are required for performance assessment considerations, would one need to explore the precipitation of the above mentioned less soluble U-bearing solids.

6.0 References

Alcorn, S. R., W. E. Coons, and M. A. Gardiner. 1990. "Estimation of Longevity of Portland Cement Grout Using Chemical Modeling Techniques." In *Scientific Basis for Nuclear Waste Management XIII*, eds. V. M. Oversby and P. W. Brown, pp. 165-173. Materials Research Society Symposium Proceedings, Volume 176, Materials Research Society, Pittsburgh, Pennsylvania.

Alcorn, S. R., J. Myers, M. A. Gardiner, and C. A. Givens. 1989. "Chemical Modeling of Cementitious Grout Materials Alteration in HLW Repositories." In *Waste Management, '89. Volume 1 - High-Level Waste and General Interest*, ed. R. G. Post, pp. 279-286. Proceedings of the Symposium on Waste Management at Tucson, Arizona, February 26 - March 2, 1989, American Nuclear Society, Inc., La Grange Park, Illinois.

Allison, J. D., D. S. Brown, and K. J. Novo-Gradac. 1991. *MINTEQA2/PRODEFA2, A Geochemical Assessment Model for Environmental Systems: Version 3.0 User's Manual.* EPA/600/3-91/021, U.S. Environmental Protection Agency, Athens, Georgia.

Atkins, M., J. Cowie, F. P. Glasser, T. Jappy, A. Kindness, and C. Pointer. 1990. "Assessment of the Performance of Cement-Based Composite Material for Radioactive Waste Immobilization." In *Scientific Basis for Nuclear Waste Management XIII*, eds. V. M. Oversby and P. W. Brown, pp. 117-127. Materials Research Society Symposium Proceedings, Volume 176, Materials Research Society, Pittsburgh, Pennsylvania.

Atkins, M., F. P. Glasser, and L. P. Moroni. 1991. "The Long-Term Properties of Cement and Concretes." In *Scientific Basis for Nuclear Waste Management XIV*, eds. T. A. Abrajano, Jr. and L. H. Johnson, pp. 373-386. Materials Research Society Symposium Proceedings, Volume 212, Materials Research Society, Pittsburgh, Pennsylvania.

Atkins, M., and F. P. Glasser. 1992. "Application of Portland Cement-Based Materials to Radioactive Waste Immobilization." *Waste Management* 12:105-131.

Atkinson, A., J. A. Herne, and C. F. Knights. 1987. *Aqueous Chemistry and Thermodynamic Modeling of CaO-SiO_2-H_2O Gels.* Report No. DOE/RW/87.048, Harwell Laboratory, Department of the Environment, Harwell, England.

Ball, J. W., E. A. Jenne, and M. W. Cantrell. 1981. *WATEQ3: A Geochemical Model with Uranium Added.* Open-File Report 81-1183, U.S. Geological Survey, Menlo Park, California.

Berner, U. R. 1987. "Modelling Porewater Chemistry in Hydrated Portland Cement." In *Scientific Basis for Nuclear Waste Management X*, eds. J. K. Bates and W. B. Seefeldt, pp. 319-330. Materials Research Society Symposium Proceedings, Volume 84, Materials Research Society, Pittsburgh, Pennsylvania.

Berner, U. R. 1988. "Modelling the Incongruent Dissolution of Hydrated Cement Minerals." *Radiochimica Acta* 44/45:387-393.

Berner, U. R. 1990. *A Thermodynamic Description of the Evolution of Pore Water Chemistry and Uranium Speciation during the Degradation of Cement.* NAGRA Technical Report 90-12, Paul Scherrer Institute, Villigen, Switzerland.

Brown, D. S., and J. D. Allison. 1987. *MINTEQA1, An Equilibrium Metal Speciation Model: User's Manual.* EPA/600/3-87/012, U.S. Environmental Protection Agency, Athens, Georgia.

Brownsword, M., A. B. Buchan, F. T. Ewart, R. McCrohon, G. J. Ormerod, J. L. Smith-Briggs, and H. P. Thomason. 1990. "The Solubility and Sorption of Uranium(VI) in a Cementitious Repository." In *Scientific Basis for Nuclear Waste Management XIII*, eds. V. M. Oversby and P. W. Brown, pp. 577-582. Materials Research Society, Volume 176, Pittsburgh, Pennsylvania.

Brush, L. H. 1980. *Solubility of Some Phases in the System UO_3-Na_2O-H_2O in Aqueous Solutions at 60°C and 90°C.* Ph.D. Dissertation, Harvard University, Cambridge, Massachusetts.

Criscenti, L. J., and R. J. Serne. 1990. "Thermodynamic Modeling of Cement/Groundwater Interactions as a Tool for Long-Term Performance Assessment." In *Scientific Basis for Nuclear Waste Management XIII*, eds. V. M. Oversby and P. W. Brown, pp. 81-89. Materials Research Society Symposium Proceedings, Volume 176, Materials Research Society, Pittsburgh, Pennsylvania.

Felmy, A. R., D. C. Girvin, and E. A. Jenne. 1984. *MINTEQ: A Computer Program for Calculating Aqueous Geochemical Equilibria.* NTIS PB84-157148 (EPA-600/3-84-032, National Technical Information Service, Springfield, Virginia.

Felmy, A. R., D. Rai, J. A. Schramke, and J. L. Ryan. 1989. "The Solubility of Plutonium Hydroxide in Dilute Solution and in High-Ionic-Strength Chloride Brines." *Radiochimica Acta* 48: 29-35.

Felmy, A. R., D. Rai, and R. W. Fulton. 1990. "The Solubility of $AmOHCO_3$(c) and the Aqueous Thermodynamics of the System Na^+-Am^{3+}-HCO_3^--OH^--H_2O." *Radiochimica Acta* 50:193-204.

Felmy, A. R., D. Rai, and M. J. Mason. 1991. "The Solubility of Hydrous Thorium (IV) Oxide in Chloride Media: Development of an Aqueous Ion-Interaction Model." *Radiochimica Acta* 55:177-185.

Felmy, A. R. and D. Rai. 1992. "An Aqueous Thermodynamic Model for a High Valence 4:2 Electrolyte Th^{4+}-SO_4^{2-} in the System Na^+-K^+-Li^+-NH_4^+-Th^{4+}-SO_4^{2-}-HSO_4^--H_2O to High Concentration." *Journal of Solution Chemistry* 21:407-423.

Felmy, A. R., D. Rai, and M. J. Mason. 1993. "Solid Phase Precipitates and Anionic Aqueous Thorium Fluoride Complexes in the Na-NH_4-Th-F-H_2O System to High Concentration." *Radiochimica Acta* 62:133-139.

Freeze, R. A. and J. A. Cherry. 1979. *Groundwater.* Prentice-Hall, Inc., Englewood Cliffs, New Jersey.

Gardiner, M. A., S. R. Alcorn, J. Myers, and C. A. Givens. 1989. "Modeling Simple Cement-Water System Using the Speciation/ Solubility/Reaction Path Computer Codes EQ3NR/EQ6, with Specific Application to Nuclear Waste Repositories." *Proceedings of the 6th International Symposium on Water-Rock Interaction*, ed. D. L. Miles, pp. 235-238. A. A. Balema, Rotterdam, Netherlands.

Glasser, F. P., D. E. Macphee, and E. E. Lachowski. 1988. "Modelling Approach to the Prediction of Equilibrium Phase Distribution in Slag-Cement Blends and Their Solubility Properties." In *Scientific Basis for Nuclear Waste Management XI*, eds. M. J. Apted and R. E. Westerman, pp. 3-12. Materials Research Society Symposium Proceedings, Volume 112, Materials Research Society, Pittsburgh, Pennsylvania.

Grenthe, I., J. Fuger, R. J. M. Konings, R. J. Lemire, A. B. Muller, C. Nguyen-Trung, and H. Wanner. 1992. *Chemical Thermodynamics Series, Volume 1: Chemical Thermodynamics of Uranium*. North-Holland, Elsevier Science Publishing Company, Inc., New York, New York.

Grenthe, I., J. Fuger, R. J. Lemire, A. B. Muller, C. Nguyen-Trung, and H. Wanner. 1990. *NEA-TDB: Chemical Thermodynamics of Uranium. Final Draft Report*. OECD Nuclear Energy Agency (NEA), Thermochemical Data Base Project Report, Final Draft Report, Paris, France.

Haworth, A., S. M. Sharland, and C. J. Tweed. 1989. "Modelling of the Degradation of Cement in a Nuclear Waste Repository," In *Scientific Basis for Nuclear Waste Management XII*, eds. W. Lutze and R. C. Ewing, pp. 447-454. Materials Research Society Symposium Proceedings, Volume 127, Materials Research Society, Pittsburgh, Pennsylvania.

Haworth, A., S. M. Sharland, and C. J. Tweed. 1990. "Modelling of the Evolution of Porewater Chemistry in a Cementitious Repository," In *Scientific Basis for Nuclear Waste Management XIII*, eds. V. M. Oversby and P. W. Brown, pp. 175-181. Materials Research Society Symposium Proceedings, Volume 176, Materials Research Society, Pittsburgh, Pennsylvania.

Hemingway, B. S. 1982. *Thermodynamic Properties of Selected Uranium Compounds and Aqueous Species at 298.15 K and 1 Bar and at Higher Temperatures--Preliminary Models for the Origins of Coffinite Deposits*. U.S. Geological Open File Report USGS-OFR-82-619, U.S. Geological Survey, Reston, Virginia.

Krupka, K. M., D. Rai, R. W. Fulton, and R. G. Strickert. 1985. "Solubility Data for U(VI) Hydroxide and Np(IV) Hydrous Oxide: Application of MCC-3 Methodology." In *Scientific Basis for Nuclear Waste Management VIII*, eds. C. M. Jantzen, J. A. Stone, and R. C. Ewing, pp. 753-760. Materials Research Society Symposium Proceedings, Volume 44, Materials Research Society, Pittsburgh, Pennsylvania.

Lea, F. M. 1988. *The Chemistry of Cement and Concrete*. Third Edition, Edward Arnold Ltd., London, United Kingdom.

Langmuir, D. 1978. "Uranium Solution-Mineral Equilibria at Low Temperatures with Applications to Sedimentary Ore Deposits." *Geochimica et Cosmochimica Acta* 42:547-569.

Nguyen, S. N., R. J. Silva, H. C. Weed, and J. E. Andrews, Jr. 1992. "Standard Gibbs Free Energies of Formation at the Temperature 303.15 K of Four Uranyl Silicates: Soddyite, Uranophane, Sodium Boltwoodite, and Sodium Weeksite." *Journal of Chemical Thermodynamics* 24:359-376.

O'Hare, P. A. G., B. M. Lewis, and S. N. Nguyen. 1988. *Thermochemistry of Uranium Compounds, XVII. Standard Molar Enthalpy of Formation at 298.15 K of Dehydrated Schoepite $UO_3 \cdot 0.9H_2O$. Thermodynamics of Schoepite + Dehydrated Schoepite + Water.* UCRL-21053 s/c 610-007. Lawrence Livermore National Laboratory, Livermore, California.

Owens, B. B., and S. W. Mayer. 1964. "The Thermodynamic Properties of Uranyl Sulphate." *Journal of Inorganic Nuclear Chemistry* 26:501-507.

Parkhurst, D. L., D. C. Thorstenson, and L. N. Plummer. 1980. *PHREEQE - A Computer Program for Geochemical Calculations.* U.S. Geological Survey Water Research Investigation 80-96, Reston, Virginia.

Peterson, S. R., C. J. Hostetler, W. J. Deutsch, and C. E. Cowan. 1987. *MINTEQ User's Manual.* NUREG/CR-4808 (PNL-6106), Pacific Northwest Laboratory, Richland, Washington.

Pitzer, K. S. 1991. "Chapter 3: Ion Interaction Approach: Theory and Data Collection." In *Activity Coefficients in Electrolyte Solutions, 2nd Edition,* ed. K. S. Pitzer, pp 75-153. CRC Press, Inc., Boca Raton, Florida.

Rai, D., A. R. Felmy, and R. W. Fulton. 1992. "Solubility and Ion Activity Product of $AmPO_4 \cdot xH_2O$ (am)." *Radiochimica Acta* 56:7-14.

Reardon, E. J. 1992. "Problems and Approaches to the Prediction of the Chemical Composition in Cement/Water Systems." *Waste Management* 12:221-239.

Rickard, D. T., and J. O. Nriagu. 1978. "Aqueous Environmental Chemistry of Lead." In *The Biochemistry of Lead in the Environment. Part A. Ecological Cycles,* ed. J. O. Nriagu, pp. 219-284. Elsevier/North-Holland Biomedical Press, New York, New York.

Roy, R. N., K. M. Vogel, C. E. Good, W. B. Davis, L. N. Roy, D. A. Johnson, A. R. Felmy, and K. S. Pitzer. 1992. "Activity Coefficients in Electrolyte Mixtures: HCl + $ThCl_4$ + H_2O for 5-55°C." *Journal of Physical Chemistry* 96:11065-11072.

Schramke, J. A., C. J. Hostetler and R. L. Erikson. 1992. *User's Guide to CTM and PRESCRNI.* PNL-9402, Pacific Northwest Laboratory, Richland, Washington.

Serne, R. J., J. L. Conca, V. L. LeGore, K. J. Cantrell, C. W. Lindenmeier, J. A. Campbell, J. E. Amonette, and M. I. Wood. 1993. *Solid-Waste Leach Characteristics and Contaminant-Sediment Interactions. Volume 1: Batch Leach and Adsorption Test and Sediment Characterization.* PNL-8889 Volume 1, Pacific Northwest Laboratory, Richland, Washington.

Serne, R. J., W. J. Martin, V. L. LeGore, C. W. Lindenmeier, S. B. McLaurine, P. F. C. Martin, and R. O. Lokken. 1989. *Leach Tests on Grouts Made with Actual and Trace Metal-Spiked Synthetic Phosphate/Sulfate Waste*. PNL-7121, Pacific Northwest Laboratory, Richland, Washington.

Sverjensky, D. A. 1990. "Progress Report for Geochemical Investigations of Uranium Mobility in the Koongarra Ore Deposit - A Natural Analogue for the Migration of Radionuclides from a Nuclear Waste Repository." In *Alligator Rivers Analogue Project Progress Report: 1 September 1989 - 30 November 1989*, ed. P. Duerden, pp. 35-40. Australian Nuclear Science and Technology Organisation, Menai, Australia.

Tripathi, V. S. 1984. *Uranium(VI) Transport Modeling: Geochemical Data and Submodels*. Ph.D. Dissertation, Stanford University, Stanford, California.

Wagman, D. D., W. H. Evans, V. B. Parker, R. H. Shumm, I. Halow, S. M. Bailey, K. L. Churney, and R. L. Nuttall. 1982. "The NBS Tables of Chemical Thermodynamic Properties. Selected Values for Inorganic and C1 and C2 Organic Substances in SI Units." *Journal of Physical and Chemical Reference Data* 11(Supplement No. 2):1-392.

Westall, J. C., J. L. Zachary, and F. M. M. Morel. 1976. *MINEQL, A Computer Program for the Calculation of Chemical Equilibrium Composition of Aqueous Systems*. Technical Note 18, Department of Civil Engineering, Massachusetts Institute of Technology, Cambridge, Massachusetts.

Appendix

MINTEQA2 Thermodynamic Database for Uranium

Appendix

MINTEQA2 Thermodynamic Database for Uranium

This appendix lists the U-bearing aqueous species and solid compounds that are in the MINTEQA2 thermodynamic database. The thermodynamic data for the U-bearing aqueous species and solids were taken primarily from Grenthe et al. (1992) and earlier drafts of this compilation and several secondary sources as noted.

Table A.1. Formula of the U-Bearing Aqueous Species and the Sources of Their Thermodynamic Data Used in MINTEQA2 Calculations

Formula	Reference Source	Formula	Reference Source
U^{3+}	Grenthe et al. (1992)	UO_2Cl^+	Grenthe et al. (1992)
U^{4+}	Grenthe et al. (1992)	$UO_2Cl_2^\circ$ (aq)	Grenthe et al. (1992)
UO_2^+	Grenthe et al. (1992)	UBr^{3+}	Grenthe et al. (1992)
UO_2^{2+}	Grenthe et al. (1992)	UO_2Br^+	Grenthe et al. (1992)
UOH^{3+}	Grenthe et al. (1992)	UI^{3+}	Grenthe et al. (1992)
$U(OH)_2^{2+}$	Grenthe et al. (1990)	USO_4^{2+}	Grenthe et al. (1992)
$U(OH)_3^+$	Grenthe et al. (1990)	$UO_2SO_4^\circ$ (aq)	Grenthe et al. (1992)
$U(OH)_4^\circ$ (aq)	Grenthe et al. (1990)	$U(SO_4)_2^\circ$ (aq)	Grenthe et al. (1992)
$U(OH)_5^-$	Grenthe et al. (1990)	$UO_2(SO_4)_2^{2-}$	Grenthe et al. (1992)
UO_2OH^+	Grenthe et al. (1992)	UNO_3^{3+}	Grenthe et al. (1992)
$UO_2(OH)_2^\circ$ (aq)	Grenthe et al. (1992)	$U(NO_3)_2^{2+}$	Grenthe et al. (1992)
$UO_2(OH)_3^-$	Grenthe et al. (1992)	$UO_2NO_3^+$	Grenthe et al. (1992)
$UO_2(OH)_4^{2-}$	Grenthe et al. (1992)	$UO_2PO_4^-$	Grenthe et al. (1990)
$(UO_2)_2OH^{3+}$	Grenthe et al. (1992)	$UO_2HPO_4^\circ$ (aq)	Grenthe et al. (1990)
$(UO_2)_2(OH)_2^{2+}$	Grenthe et al. (1992)	$UO_2H_2PO_4^+$	Grenthe et al. (1990)
$(UO_2)_3(OH)_4^{2+}$	Grenthe et al. (1992)	$UO_2H_3PO_4^{2+}$	Grenthe et al. (1990)
$(UO_2)_3(OH)_5^+$	Grenthe et al. (1992)	$UO_2(H_2PO_4)_2^\circ$ (aq)	Grenthe et al. (1990)
$(UO_2)_3(OH)_7^-$	Grenthe et al. (1992)	$UO_2(H_2PO_4)(H_3PO_4)^+$	Grenthe et al. (1990)
$(UO_2)_4(OH)_7^+$	Grenthe et al. (1992)	$U(CO_3)_4^{4-}$	Grenthe et al. (1992)
$U_6(OH)_{15}^{9+}$	Grenthe et al. (1992)	$U(CO_3)_5^{6-}$	Grenthe et al. (1992)
UF^{3+}	Grenthe et al. (1992)	$UO_2CO_3^\circ$ (aq)	Grenthe et al. (1992)
UF_2^{2+}	Grenthe et al. (1992)	$UO_2(CO_3)_2^{2-}$	Grenthe et al. (1992)
UF_3^+	Grenthe et al. (1992)	$UO_2(CO_3)_3^{4-}$	Grenthe et al. (1992)
UF_4° (aq)	Grenthe et al. (1992)	$UO_2(CO_3)_3^{5-}$	Grenthe et al. (1992)
UF_5^-	Grenthe et al. (1992)	$(UO_2)_3(CO_3)_6^{6-}$	Grenthe et al. (1992)
UF_6^{2-}	Grenthe et al. (1992)	$UO_2OHCO_2^+$	Grenthe et al. (1990)
UO_2F^+	Grenthe et al. (1992)	$(UO_2)_{11}(CO_3)_6(OH)_{12}^{2-}$	Grenthe et al. (1990)
$UO_2F_2^\circ$ (aq)	Grenthe et al. (1992)	$(UO_2)_2CO_3(OH)_3^-$	Grenthe et al. (1990)
$UO_2F_3^-$	Grenthe et al. (1992)	$UO_2SiO(OH)_3^+$; same as $UO_2H_3SiO_4^+$	Grenthe et al. (1990)
$UO_2F_4^{2-}$	Grenthe et al. (1992)		
UCl^{3+}	Grenthe et al. (1992)		

Table A.2. Formula and Mineral Names of the U-Bearing Solid Compounds and the Sources of Their Thermodynamic Data Used in MINTEQA2 Calculations

Formula	Mineral Name	Reference Source
UBr_2Cl		Grenthe et al. (1990)
UBr_3		Grenthe et al. (1990)
UCl_3		Grenthe et al. (1990)
$UBrCl_2$		Grenthe et al. (1990)
UOCl		Grenthe et al. (1990)
UF_3		Grenthe et al. (1990)
UI_3		Grenthe et al. (1990)
UO_2 (am)		Grenthe et al. (1990)
U_4O_9		Langmuir (1978)
U_3O_8		Grenthe et al. (1990)
UBr_4		Grenthe et al. (1990)
$UOBr_2$		Grenthe et al. (1990)
UBr_3Cl		Grenthe et al. (1990)
$UBrCL_3$		Grenthe et al. (1990)
UCl_4		Grenthe et al. (1990)
UBr_2Cl_2		Grenthe et al. (1990)
$UOCl_2$		Grenthe et al. (1990)
$U_2O_2Cl_5$		Grenthe et al. (1990)
UF_4		Grenthe et al. (1990)
$UF_4 \cdot 2.5H_2O$		Grenthe et al. (1990)
U_2F_9		Grenthe et al. (1990)
U_4F_{17}		Grenthe et al. (1989)
$UClF_3$		Grenthe et al. (1990)
UCl_2F_2		Grenthe et al. (1990)
UCl_3F		Grenthe et al. (1990)
UOF_2		Grenthe et al. (1990)
$UOF_2 \cdot H_2O$		Grenthe et al. (1990)
UOFOH		Grenthe et al. (1990)
UI_4		Grenthe et al. (1990)
$UClI_3$		Grenthe et al. (1990)
UCl_2I_2		Grenthe et al. (1990)
UCl_3I		Grenthe et al. (1990)
$U(CO_3)_2$		Grenthe et al. (1990)
$U(OH)_2SO_4$		Grenthe et al. (1990)
$U(SO_4)_2$		Grenthe et al. (1990)
$U(SO_4)_2 \cdot 4H_2O$		Grenthe et al. (1990)
$U(SO_4)_2 \cdot 8H_2O$		Grenthe et al. (1990)
$U(HPO_4)_2 \cdot 4H_2O$		Grenthe et al. (1990)
$USiO_4$	Coffinite	Grenthe et al. (1990)
Na_3UO_4		Grenthe et al. (1990)
UBr_5		Grenthe et al. (1990)

Table A.2. (continued)

Formula	Mineral Name	Reference Source
$UOBr_3$		Grenthe et al. (1990)
UCl_5		Grenthe et al. (1990)
$UOCl_3$		Grenthe et al. (1990)
UO_2Cl		Grenthe et al. (1990)
$U_5O_{12}Cl$		Grenthe et al. (1990)
α-UF_5		Grenthe et al. (1990)
β-UF_5		Grenthe et al. (1990)
UPO_5		Grenthe et al. (1990)
β-$UO_2(OH)_2$		Grenthe et al. (1990)
$UO_3 \cdot 2.0H_2O$	Schoepite	Grenthe et al. (1990)
$UO_3 \cdot 0.393H_2O$	Dehyrated Schoepite	O'Hare et al. (1988)
$UO_3 \cdot 0.648H_2O$	Dehyrated Schoepite	O'Hare et al. (1988)
$UO_3 \cdot 0.850H_2O$	Dehyrated Schoepite	O'Hare et al. (1988)
$UO_3 \cdot 0.900H_2O$	Dehyrated Schoepite	Grenthe et al. (1990)
$UO_3 \cdot 1.000H_2O$	Dehyrated Schoepite	O'Hare et al. (1988)
UO_2	Uraninite	Grenthe et al. (1990)
α-UO_3		Grenthe et al. (1990)
β-UO_3		Grenthe et al. (1990)
γ-UO_3		Grenthe et al. (1990)
UO_3 (am)	Gummite	Langmuir (1978)
K_2UO_4		Grenthe et al. (1990)
Li_2UO_4		Grenthe et al. (1990)
$Na_2U_2O_7$		Grenthe et al. (1990)
α-Na_2UO_4		Grenthe et al. (1990)
$BaUO_4$		Grenthe et al. (1990)
$CaUO_4$		Grenthe et al. (1990)
$MgUO_4$		Grenthe et al. (1990)
$NaUO_3$		Grenthe et al. (1990)
$NaUO_2(CO_3)_3$		Grenthe et al. (1990)
Rb_2UO_4		Grenthe et al. (1990)
α-$SrUO_4$		Grenthe et al. (1990)
UO_2Br_2		Grenthe et al. (1990)
$UO_2Br_2 \cdot H_2O$		Grenthe et al. (1990)
$UO_2Br_2 \cdot 3H_2O$		Grenthe et al. (1990)
$UO_2BrOH \cdot 2H_2O$		Grenthe et al. (1990)
UCl_6		Grenthe et al. (1990)
UO_2Cl_2		Grenthe et al. (1990)
$UO_2Cl_2 \cdot H_2O$		Grenthe et al. (1990)
$UO_2Cl_2 \cdot 3H_2O$		Grenthe et al. (1990)
$UO_2ClOH \cdot 2H_2O$		Grenthe et al. (1990)
$(UO_2)_2Cl_3$		Grenthe et al. (1990)
UF_6		Grenthe et al. (1990)

Table A.2. (continued)

Formula	Mineral Name	Reference Source
UO_2FOH		Grenthe et al. (1990)
$UO_2FOH \cdot H_2O$		Grenthe et al. (1990)
$UO_2FOH \cdot 2H_2O$		Grenthe et al. (1990)
UO_2F_2		Grenthe et al. (1990)
$UO_2F_2 \cdot 3H_2O$		Grenthe et al. (1990)
$U_2O_3F_6$		Grenthe et al. (1990)
$U_3O_5F_8$		Grenthe et al. (1990)
UOF_4		Grenthe et al. (1990)
UO_2CO_3	Rutherfordine	Grenthe et al. (1990)
$UO_2(NO_3)_2$		Grenthe et al. (1990)
$UO_2(NO_3)_2 \cdot H_2O$		Grenthe et al. (1990)
$UO_2(NO_3)_2 \cdot 2H_2O$		Grenthe et al. (1990)
$UO_2(NO_3)_2 \cdot 3H_2O$		Grenthe et al. (1990)
$UO_2(NO_3)_2 \cdot 6H_2O$		Grenthe et al. (1990)
UO_2SO_4		Grenthe et al. (1990)
$UO_2SO_4 \cdot H_2O$		Owens and Mayer (1964)
$UO_2SO_4 \cdot 2.5H_2O$		Owens and Mayer (1964)
$UO_2SO_4 \cdot 3H_2O$		Owens and Mayer (1964)
$UO_2SO_4 \cdot 3.5H_2O$		Owens and Mayer (1964)
$(UO_2)_3(PO_4)_2$		Grenthe et al. (1990)
$(UO_2)_3(PO_4)_2 \cdot 4H_2O$		Grenthe et al. (1990)
$(UO_2)_2P_2O_7$		Grenthe et al. (1990)
$Pb_2(UO_2)(PO_4)_2 \cdot 2H_2O$	Parsonite	Rickard and Nriagu (1978)
$UO_2(PO_3)_2$		Grenthe et al. (1990)
UO_2HPO_4		Tripathi (1984)
$UO_2HPO_4 \cdot 4H_2O$		Grenthe et al. (1990)
$UP_2O_7 \cdot 20H_2O$		Grenthe et al. (1990)
$UO_2(AsO_3)_2$		Grenthe et al. (1990)
$(UO_2)_2As_2O_7$		Grenthe et al. (1990)
$(UO_2)_3(AsO_4)_2$		Grenthe et al. (1990)
$K(UO_2)AsO_4$		Wagman et al. (1982)
$K(H_3O)(UO_2)(SiO_4)$	Boltwoodite	Hemingway (1982)
$Ca(UO_2)_2(Si_2O_5)_3 \cdot 5H_2O$	Haiweeite	Hemingway (1982)
$Pb(UO_2)_2SiO_4 \cdot H_2O$	Kasolite	Hemingway (1982)
$Mg(H_3O)_2(UO_2)_2(SiO_4)_2 \cdot 4H_2O$	Sklodowskite	Hemingway (1982)
$(UO_2)_2(SiO_4) \cdot 2H_2O$	Soddyite	Hemingway (1982)
$K_2(UO_2)_2(Si_2O_5)_3 \cdot 4H_2O$	Weeksite	Hemingway (1982)
$Ca(UO_2)_2(VO_4)_2$	Tyuyamunite	Langmuir (1978)
$K(UO_2)(VO_4)$	Carnotite	Langmuir (1978)
$Ca(UO_2)_2(PO_4)_2$	Autunite	Sverjensky (1990)
$H_2(UO_2)_2(PO_4)_2$	H-Autunite	Grenthe et al. (1990)
$K_2(UO_2)_2(PO_4)_2$	K-Autunite	Sverjensky (1990)

Table A.2. (continued)

Formula	Mineral Name	Reference Source
$Na_2(UO_2)_2(PO_4)_2$	Na-Autunite	Sverjensky (1990)
$Sr(UO_2)_2(PO_4)_2$	Sr-Autunite	Langmuir (1978)
$CaU(PO_4)_2 \cdot 2H_2O$	Ningoyite	Langmuir
(1978)$(NH_4)_2(UO_2)_2(PO_4)_2$	Uramphite	Langmuir (1978)
$Mg(UO_2)_2(PO_4)_2$	Saleeite	Sverjensky (1990)
$Ba(UO_2)_2(PO_4)_2$	Uranocirite	Langmuir (1978)
$Fe(UO_2)_2(PO_4)_2$	Bassetite	Langmuir (1978)
$Ca(UO_2)_2(PO_4)_2$	Torbernite	Sverjensky (1990)
$Pb(UO_2)_2(PO_4)_2$	Przhevalskite	Langmuir (1978)
$Ca(UO_2)_2(SiO_3OH)_2$	Uranophane	Nguyen et al. (1992)

Distribution

No. of Copies

OFFSITE

12 DOE/Office of Scientific and Technical Information

J. A. Coleman, NE-24
DOE Office of Remedial Action and Waste Technology
19901 Germantown Road
Germantown, MD 20545

2 Westinghouse Savannah River Company
Savannah River Site
Aiken, SC 29808-001
Attn: C. A. Langton
E. Wilhite

2 Brookhaven National Laboratory
Upton, NY 19973
Attn: M. Fuhrmann
T. M. Sullivan

4 Nuclear Regulatory Commission
Office of Nuclear Regulatory Research
Washington, DC 20555
Attn: A. C. Campbell
J. W. Bradbury
E. O'Donnell
P. R. Reed

2 Oak Ridge National Laboratory
P. O. Box X
Oak Ridge, TN 37831
Attn.: T. M. Gilliam
R. Spence

No. of Copies

2 EG&G
P. O. Box 1625
Idaho Falls, ID 83415
Attn.: J. McConnell
R. Rogers

T. L. Jones
New Mexico State University
Dept. of Agronomy
Agriculture Building
Room 254
Los Cruces, NM 88003-003

FOREIGN

A. Atkinson
Atomic Energy Research Establishment
Harwell
Didcot
Oxfordshire OX 11 ORA
UNITED KINGDOM

L. P. Buckley
Atomic Energy of Canada Ltd.
Chalk River, Ontario K0J 1J0
CANADA

R. Dayal
Ontario Hydro
800 Kipling Ave.
Toronto, Ontario M8Z 5S4
CANADA

J. H. Rowat
Atomic Energy of Canada Ltd.
Chalk River Laboratories
Mail Station 15
Chalk River, Ontario
CANADA KOJ 1JO

No. of Copies

ONSITE

3 **DOE Richland Operations Office**

D. H. Alexander S7-51
R. D. Freeberg A5-19
R. F. Guercia S7-55

13 **Westinghouse Hanford Company**

K. C. Burgard G6-13
K. L. Hladek T4-02
F. N. Hodges G1-40
F. M. Mann H0-36
J. W. Shade H5-27
J. C. Sonnichsen H6-23
J. L. Westcott T3-04
M. I. Wood (5) T4-02
G. F. Williamson G6-13

Washington State University-TriCities
J. A. Conca H2-52

No. of Copies

38 **Pacific Northwest Laboratory**

K. J. Cantrell K6-81
L. J. Criscenti (5) K6-81
G. W. Gee K9-33
G. R. Holdren K6-81
D. I. Kaplan K6-81
C. T. Kincaid K9-33
K. M. Krupka (5) K6-81
V. L. Legore P8-37
C. W. Lindenmeier K6-81
R. O. Lokken P8-37
P.F.C. Martin P8-37
W. J. Martin K1-19
S. V. Mattigod K6-81
R. J. Serne (10) K6-81
G. A. Whyatt P7-19
Publishing Coordination
Technical Report Files (5)

File: Cem-U-V8.doc